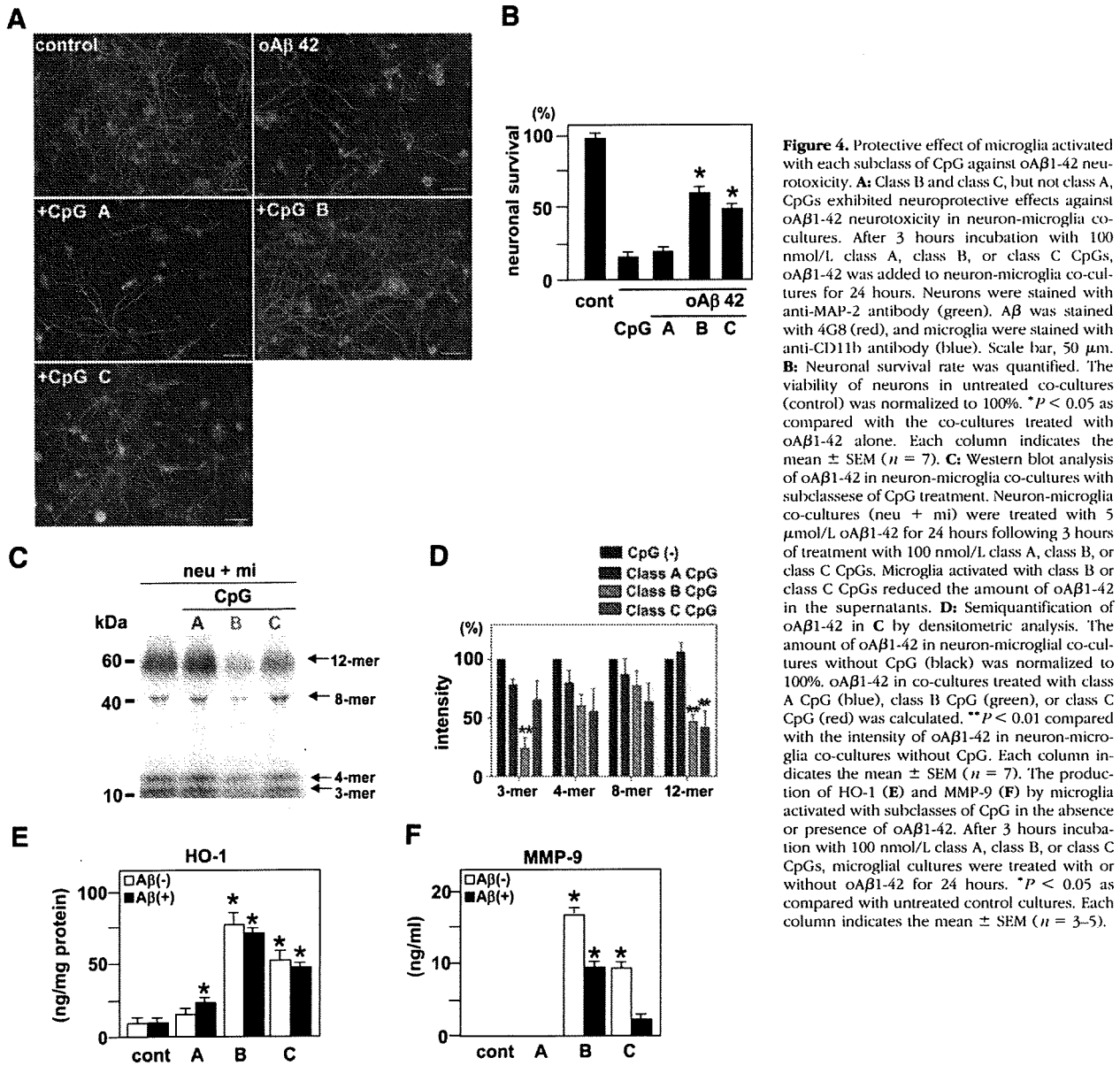

Figure 4. Protective effect of microglia activated with each subclass of CpG against oAβ1-42 neurotoxicity. **A:** Class B and class C, but not class A, CpGs exhibited neuroprotective effects against oAβ1-42 neurotoxicity in neuron-microglia co-cultures. After 3 hours incubation with 100 nmol/L class A, class B, or class C CpGs, oAβ1-42 was added to neuron-microglia co-cultures for 24 hours. Neurons were stained with anti-MAP-2 antibody (green). Aβ was stained with 4G8 (red), and microglia were stained with anti-CD11b antibody (blue). Scale bar, 50 μm. **B:** Neuronal survival rate was quantified. The viability of neurons in untreated co-cultures (control) was normalized to 100%. $^{*}P < 0.05$ as compared with the co-cultures treated with oAβ1-42 alone. Each column indicates the mean ± SEM ($n = 7$). **C:** Western blot analysis of oAβ1-42 in neuron-microglia co-cultures with subclassese of CpG treatment. Neuron-microglia co-cultures (neu + mi) were treated with 5 μmol/L oAβ1-42 for 24 hours following 3 hours of treatment with 100 nmol/L class A, class B, or class C CpGs. Microglia activated with class B or class C CpGs reduced the amount of oAβ1-42 in the supernatants. **D:** Semiquantification of oAβ1-42 in **C** by densitometric analysis. The amount of oAβ1-42 in neuron-microglial co-cultures without CpG (black) was normalized to 100%. oAβ1-42 in co-cultures treated with class A CpG (blue), class B CpG (green), or class C CpG (red) was calculated. $^{**}P < 0.01$ compared with the intensity of oAβ1-42 in neuron-microglia co-cultures without CpG. Each column indicates the mean ± SEM ($n = 7$). The production of HO-1 (**E**) and MMP-9 (**F**) by microglia activated with subclasses of CpG in the absence or presence of oAβ1-42. After 3 hours incubation with 100 nmol/L class A, class B, or class C CpGs, microglial cultures were treated with or without oAβ1-42 for 24 hours. $^{*}P < 0.05$ as compared with untreated control cultures. Each column indicates the mean ± SEM ($n = 3$–5).

neuroprotection of CpG. Furthermore, treatment of oAβ significantly increased ROS production in the neuron microglia co-cultures. Pretreatment of 100 nmol/L CpG significantly suppressed ROS production by oAβ (Figure 3G).

Although TLR4 ligand lipopolysaccharide generally increases microglial production of neurotoxic molecules including TNF-α, nitrite and glutamate; 100 nmol/L CpG did not induce these toxic molecules in microglia (Figure 3H).

Microglia Activated with Class B and C, but not Class A CpG, Attenuate oAβ1-42 Neurotoxicity

CpG ODNs are divided into three classes by their ability to induce IFN-α expression in plasmacytoid dendritic cells (class A) and to promote survival, activation, and maturation of B cells and plasmacytoid dendritic cell (class B) or both (class C)[30]. We examined which class of CpG induces the neuroprotective effects of microglia. Class A CpG neither activated microglia nor induced neuroprotective effects against oAβ1-42 toxicity, whereas both class B and C CpGs activated microglia and significantly increased neuronal survival, to 58 and 49% following oAβ1-42 treatment, respectively (Figures 4, A and B). Western blot analysis revealed that class B CpG significantly decreased the amount of trimers and dodecamers of oAβ1-42 present in the supernatants of neuron-microglia co-cultures, and class C CpG significantly decreased dodecamers of oAβ1-42, whereas oAβ1-42 did not decrease by the administration of class A CpG (Figure 4, C and D). In addition, microglia activated with class B and C CpGs expressed HO-1 in both the absence or presence of oAβ1-42, whereas treatment with class A CpG only slightly increased HO-1 expression in the pres-

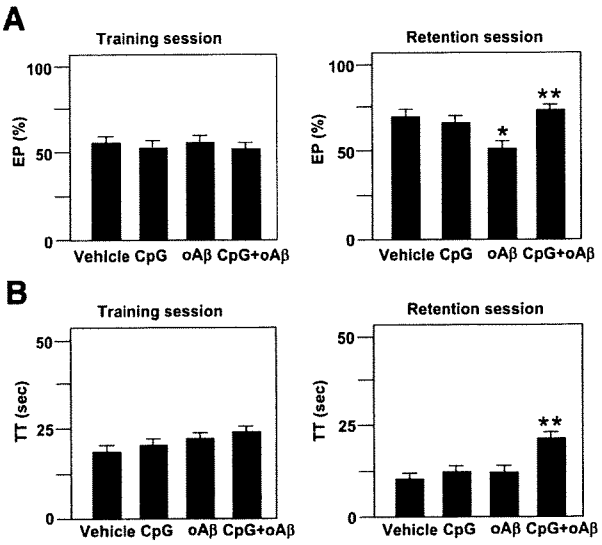

Figure 5. Effect of ICV injection of CpG on oAβ1-42-induced cognitive impairment in the NORT. **A:** Exploratory preference (EP) and total exploring time (TT) (**B**) in the training session (**left**) and the retention session (**right**). NORT was performed 7 to 8 days after ICV injection of oAβ1-42. Each column indicates the mean ± SEM (n = 6–7). $^{*}P < 0.05$ as compared with controls. $^{**}P < 0.05$ as compared with oAβ1-42-injected mice.

ence of oAβ1-42 (Figure 4E). Microglia activated with class B and C CpGs also produced MMP-9 (Figures 4F).

ICV Injection of CpG Ameliorates oAβ-Induced Impairment of Recognition Memory in the NORT

To examine the role of CpG-activated microglia in cognitive dysfunction induced by oAβ1-42, we investigated the effect of *in vivo* administration of CpG on the impairment of recognition memory in the NORT after ICV injection of oAβ1-42. Mice injected with oAβ1-42 displayed significantly reduced exploratory preference for the novel object in the retention session ($F_{(3,21)} = 3.68$, $P < 0.05$; Figure 5A), although total exploration time in the training and retention sessions was unaffected. The result implies that oAβ1-42 induces the impairment of recognition memory. Simultaneous injection of CpG with oAβ1-42 significantly improved both exploratory preference ($F_{(3,21)} = 3.68$, $P < 0.05$; Figure 5A) and total exploration time ($F_{(3,21)} = 4.41$, $P < 0.05$; Figure 5B) in the retention session, although exploratory preference and total exploration time were unaffected in the training session. .

ICV Injection of CPG Ameliorates the Impairment of Associative Learning in the Cued and Contextual Fear-Conditioning Tests in Tg2576 Mice

Next, we examined the effect of CpG on the cognitive function of Tg2576 mouse model of AD. We evaluated associative learning at the age of 10 months in a conditioned fear learning test. In the preconditioning phase (training), the mice hardly showed any freezing response. There were no differences in basal levels of freezing response between the groups (data not shown). In the contextual learning test, wild-type mice showed a marked contextual freezing response 24 hours after fear conditioning (Figure 6A). However, vehicle-injected Tg2576 mice exhibited less of a freezing response in the contextual tests (Figure 6A), indicating an impairment of associative learning. The CpG (10 or 100 nmol/L)-injected Tg2576 mice were indistinguishable from wild-type mice, and the CpG treatment dose-dependently and significantly reversed the contextual freezing response as compared with vehicle-injected Tg2576 mice ($F_{(3,35)} = 9.54$, $P < 0.05$; Figure 6A). In the cued (tone) learning test, although there was no significant difference in the cued freezing response at 24 hours after fear conditioning between wild-type and vehicle-injected Tg2576 mice, both injection of 10 and 100 nmol/L CpG showed a tendency to reverse the cued freezing response (Figure 6B). No alterations of nociceptive response were found in any of the mutant mice: there was no difference in the minimal current required to elicit flinching/running, jumping, or vocalization among the mice (data not shown). Then, we examined whether CpG decreased Aβ deposits in the cortex (Figure 6C) and the hippocampus (Figure 6D) of Tg 2576 mice. No Aβ deposits were seen in wild-type mice. Although Aβ deposits (green) were abundant in the cortex and the hippocampus of vehicle-injected Tg2576 mice, ICV injection of CpG significantly decreased Aβ deposits in both areas. Microglia (red) clustered around Aβ deposits (Figure 6, C and D). CpG decreased Aβ load in a significant, dose-dependent manner in both areas (Figure 6E). We examined oAβ in the soluble, extracellular-enriched fractions of the hemi-forebrains of mice and detected 12-mer oAβ in vehicle-injected Tg2576 mice by Western blotting. The 12-mer oAβ was strikingly and significantly decreased in 100 nmol/L CpG-injected Tg2576 mice (Figure 6, F and G).

Discussion

Recent studies have proposed that oAβ1-42 contributes to the neurotoxicity associated with AD. AD begins with subtle alterations of hippocampal synaptic efficacy before frank neuronal degeneration, and this synaptic dysfunction is caused by diffusible oAβ.[31] Disruption of hippocampal long-term potentiation and synaptic plasticity by oAβ1-42 appears to involve Ca^{2+} signaling,[32] oxidative stress mediated by an *N*-methyl-D-aspartate receptor,[4,33] and protein phosphatase 1.[34] In addition, oAβ interferes with insulin receptor function in hippocampal neurons and inhibits the activation of specific kinases required for long-term potentiation.[35] In the present study, we have confirmed that oAβ1-42 exhibits more potent neurotoxicity than fAβ1-42 in murine cortical cultures.[5,36] Therefore, decreasing or preventing formation of oAβ1-42 is a potential therapeutic strategy against AD.

The precise role of microglia in oAβ1-42 toxicity remains unclear. Microglia stimulated with Aβ are reported to release proinflammatory cytokines via the nuclear factor κB[37,38] and contribute to the pathogenesis of AD. However, in our experimental conditions, oAβ1-42 neither

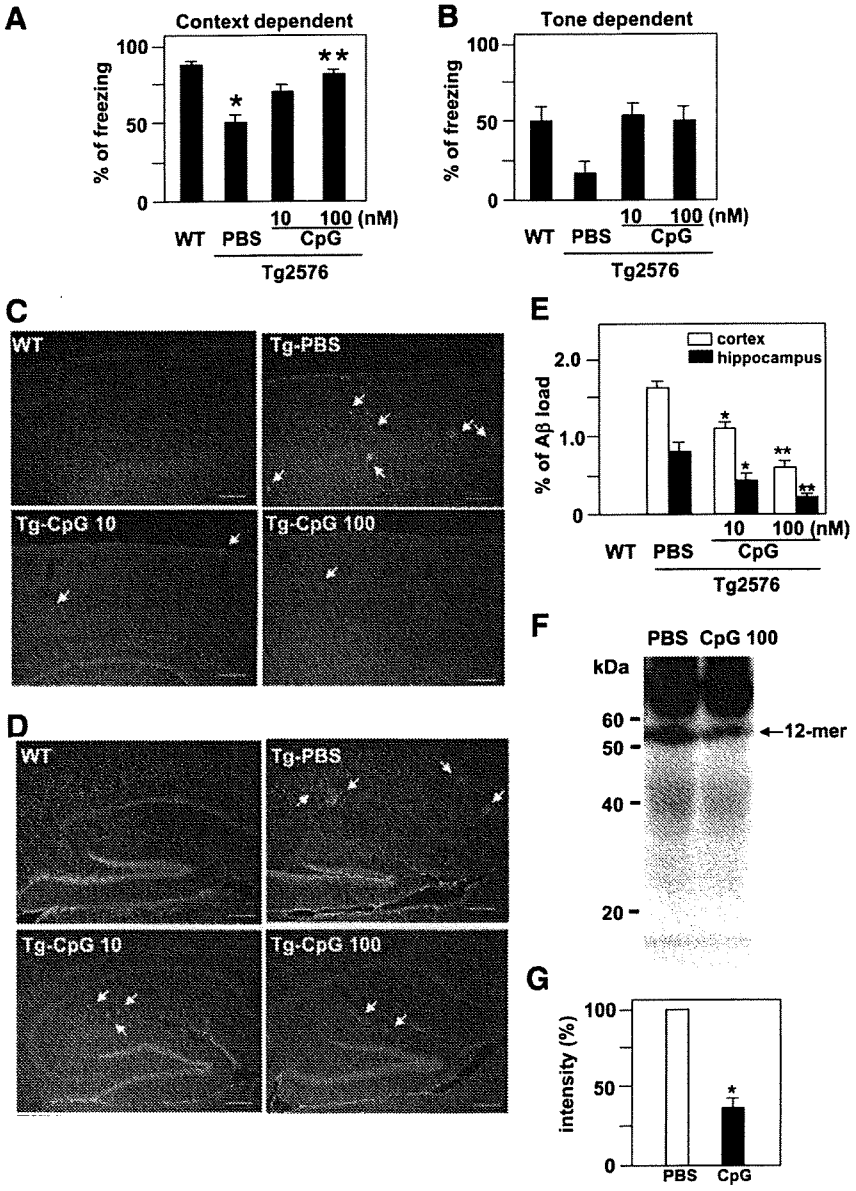

Figure 6. Effect of ICV injection of CpG on associative learning in the cued and contextual conditioning tests and Aβ clearance in Tg2576 mice. The retention session was performed 24 hours after the training. Context-dependent (**A**) and tone-dependent (**B**) freezing times were measured at the age of 10 months. Each column indicates the mean ± SEM (wild-type (WT) mice, $n = 14$; vehicle-treated (PBS) Tg2576 mice, $n = 9$; CpG (10 nmol/L)-treated Tg2576, $n = 8$; CpG (100 nmol/L)-treated Tg2576, $n = 8$). $^{*}P < 0.05$ compared with wild type. $^{**}P < 0.05$ as compared with vehicle-treated Tg2576 mice. **C:** Aβ deposits in the cortex. Aβ was stained with 4G8 (green), microglia stained with anti-CD11b antibody (red), and cell nucleus stained with Hoechst 33342 (blue). **White arrows** indicate Aβ deposits surrounding by microglia. Scale bar, 200 μm. **D:** Aβ deposits in the hippocampus. Scale bar, 200 μm. **E:** Quantification of Aβ deposits in **C** and **D**. The ratio between the Aβ deposits area and the total area of the analyzed region was multiplied by 100. $^{*}P < 0.05$ and $^{**}P < 0.01$ as compared with vehicle-treated Tg2576 mice. Each column indicates the mean ± SEM ($n = 3$). **F:** Western blot analysis of oAβ extracted from the hemi-forebrains of Tg 2576 mice. A 12-mer oAβ was detected in vehicle-treated Tg2576 mice and decreased in 100 nmol/L CpG-injected Tg2576 mice. **G:** Semi-quantification of 12-mer oAβ by densitometric analysis. The amount of 12-mer oAβ1-42 in vehicle-treated Tg2576 mice was normalized to 100%. $^{*}P < 0.05$ as compared with vehicle-treated Tg2576 mice. Each column indicates the mean ± SEM ($n = 4$).

activated microglia nor induced the release of neurotoxic proinflammatory cytokines, NO, or glutamate. These results suggest that oAβ1-42 is not acting to trigger of microglial neurotoxicity.

TLR signaling pathways contribute to phagocytosis of Aβ. TLR2 acts as an endogenous receptor for the clearance of Aβ by bone marrow-derived microglia.[9] Interestingly, a TLR4 mutation exacerbates Aβ burden in mouse models of AD.[39] Thus, we investigated whether microglia activated with TLR ligands exert neuroprotective effects against oAβ1-42 toxicity. Consequently, we found that TLR9 ligand CpG enhanced microglial neuroprotection. Furthermore, CpG exerted the neuroprotective effect of BV-2 microglial cell line against oAβ toxicity (data not shown). TLR9, which detects single-stranded DNA containing unmethylated CpG, is located in intracellular endosomal-lysosomal compartment. We confirmed that microglia expressed TLR9 at a higher level, whereas astrocytes and neuronal cells expressed it at a lower level (data not shown). Thus, CpG mainly acts on microglia in the central nervous system. TLR7 and TLR8 are closely associated with TLR9. They are also located in endosomal-lysosomal compartment and detect single-stranded RNA. The ligands for TLR7 and TLR8 may also have some roles in microglial neuroprotection.

Western blot analysis revealed that microglia activated with CpG reduced the amount of oAβ present in the supernatant of treated cultures. Moreover, CpG was a potent inducer of antioxidant enzyme HO-1. The up-regulation of HO-1 in microglia by CpG treatment may lead to neuroprotection via suppression of ROS production by oAβ. HO-1, a member of the heat-shock protein family, is a microsomal enzyme that oxidatively cleaves heme to produce biliverdin, carbon monoxide, and iron.[40] Aβ binds to heme to promote a functional heme deficiency, mitochondrial dysfunction, and neurotoxicity.[41] Amyloid

precursor protein also binds to HO, and oxidative neurotoxicity is markedly enhanced in cerebral cortical cultures from amyloid precursor protein Swedish mutant transgenic mice.[42]

HO-1 is reported to be induced by the anti-inflammatory cytokine IL-10.[29] Although CpG induced IL-10 in microglia in the absence of oAβ, IL-10 production was inhibited in the presence of oAβ. Therefore, HO-1 may be induced by a discrete mechanism independent from IL-10 in AD.

MMP-9, a protease that degrades Aβ, is expressed at higher levels in the brains of AD patients and may play an important role in amyloid clearance by degrading both oAβ and fAβ.[10] MMP-9 expression is increased by serum amyloid A through formyl peptide receptor-like-1.[43] Although CpG stimulation induced MMP-9 in microglia, inhibiting MMP-9 pharmacologically did not affect neuroprotection by microglia. Thus, MMP-9 may not mainly contribute to the neuroprotection provided by CpG-activated microglia.

In the present study, CpG induced fewer neurotoxic molecules such as TNF-α, NO, and glutamate in microglia, whereas previous studies have reported that CpG-activated microglia produce TNF-α, IL-12, and NO[44] and induce neuronal damage.[45] The discrepancies between these studies and our experiments may be a consequence of differences in the concentrations of TLR ligands used. Higher concentration (10 μmol/L) of CpG have been used for microglial activation in previous reports, whereas here we have used lower concentrations (1 to 100 nmol/L) of CpG.

In addition, we observed that the neuroprotective effect differs among CpG ODN classes. The responses of microglia to the different classes of CpG have not been fully understood. Here, we showed for the first time that class A CpG did not activate microglia, whereas class B and C CpGs induced neuroprotection by microglia that was mediated by clearance of oAβ and induction of HO-1. Three major classes of CpG ODN are structurally distinct. The structures of class A CpG include poly-G motifs at the 5′ and/or 3′ ends that are capable of forming very stable but complex higher-ordered structures and a central phosphodiester region containing one or more CpG motifs in a self-complementary palindrome. Class B CpG has a completely phosphorothioate backbone and does not form typically higher-ordered structures. Class C CpG has a phosphorothioate backbone, and 3′ palindrome forms duplex.[46] These distinct structures of CpG ODN may reflect different microglial responses.

Finally, we examined the effect of CpG on oAβ1-42 neurotoxicity in two different *in vivo* studies. The ICV administration of Aβ25-35 is reported to cause cognitive impairment in a NORT. Oxidative stress contributes to the onset of this cognitive dysfunction.[23] We found that injection of oAβ1-42 also induced cognitive impairment as assessed by NORT. Surprisingly, one-time ICV injection of CpG improved both the cognitive impairment by oAβ1-42 in NORT. The impairment of associative learning in Tg 2576 mouse model of AD was also effectively suppressed by ICV injection of CpG. We also confirmed that CpG treatment decreased Aβ deposits and oAβ in Tg 2576 mice. Our results concur with the recent study that a total of 14 i.p. injection of CpG into Tg 2576 mice beginning at the age of 6 weeks, and once a month, ameliorates AD-related pathology.[28] Aβ plaques are reported to form extraordinarily quickly, over 24 hours. Within 1 to 2 days of a new plaque's appearance, microglia are activated and recruited to the site.[47] ICV injection of CpG may directly induce microglial activation via TLR9 and enhance microglial rapid uptake of oAβ through fluid-phase macropinocytosis as reported recently.[48] CpG may also enhance microglial phagocytosis of fAβ through formyl peptide receptor-like 2.[11] Such mechanisms of Aβ clearance by CpG can decrease Aβ plaque formation in Tg 2576 mice.

Recently, the therapeutic potential of CpG has generated great interest.[46] CpG offers a potent adjuvant activity that elicits a more effective immune response to infectious agents or tumors. A previous report[49] demonstrated that CpG strongly inhibits the effector phase of inflammatory arthritis. In addition, CpG can serve as a potent preconditioning stimulus and provide protection against ischemic brain injury.[50] Our findings suggest that CpG, especially class B and C, may also be effective therapeutic agents against oAβ1-42 neurotoxicity in AD.

References

1. Busciglio J, Lorenzo A, Yeh J, Yankner BA: β-Amyloid fibrils induce tau phosphorylation and loss of microtubule binding. Neuron 1995, 14:879–888
2. Grace EA, Rabiner CA, Busciglio J: Characterization of neuronal dystrophy induced by fibrillar amyloid β: implications for Alzheimer's disease. Neuroscience 2002, 114:265–273
3. Walsh DM, Klyubin I, Fadeeva JV, Cullen WK, Anwyl R, Wolfe MS, Rowan MJ, Selkoe DJ: Naturally secreted oligomers of amyloid β protein potently inhibit hippocampal long-term potentiation in vivo. Nature 2002, 416:535–539
4. De Felice FG, Velasco PT, Lambert MP, Viola K, Fernandez SJ, Ferreira ST, Klein WL: Aβ oligomers induce neuronal oxidative stress through an *N*-methyl-D-aspartate receptor-dependent mechanism that is blocked by the Alzheimer drug memantine. J Biol Chem 2007, 282:11590–11601
5. Deshpande A, Mina E, Glabe C, Busciglio J: Different conformations of amyloid β induce neurotoxicity by distinct mechanisms in human cortical neurons. J Neurosci 2006, 26:6011–6018
6. Meda L, Cassatella MA, Szendrei GI, Otvos L Jr, Baron P, Villalba M, Ferrari D, Rossi F: Activation of microglial cells by β-amyloid protein and interferon γ. Nature 1995, 374:647–650
7. McGeer PL, McGeer EG: Inflammation, autotoxicity and Alzheimer disease. Neurobiol Aging 2001, 22:799–809
8. Mizuno T, Kurotani T, Komatsu Y, Kawanokuchi J, Kato H, Mitsuma N, Suzumura A: Neuroprotective role of phosphodiesterase inhibitor Ibudilast on neuronal cell death induced by activated microglia. Neuropharmacology 2004, 46:404–411
9. Richard KL, Filali M, Préfontaine P, Rivest S: Toll-like receptor 2 acts as a natural innate immune receptor to clear amyloid β 1-42 and delay the cognitive decline in a mouse model of Alzheimer's disease. J Neurosci 2008, 28:5784–5793
10. Yan P, Hu X, Song H, Yin K, Bateman RJ, Cirrito JR, Xiao Q, Hsu FF, Turk JW, Xu J, Hsu CY, Holtzman DM, Lee JM: Matrix metalloproteinase-9 degrades amyloid-β fibrils in vitro and compact plaques in situ. J Biol Chem 2006, 281:24566–24574
11. Iribarren P, Chen K, Hu J, Gong W, Cho EH, Lockett S, Uranchimeg B, Wang JM: CpG-containing oligodeoxynucleotide promotes microglial cell uptake of amyloid β 1-42 peptide by up-regulating the expression of the G-protein-coupled receptor mFPR2. FASEB J 2005, 19:2032–2034

12. Chen K, Iribarren P, Hu J, Chen J, Gong W, Cho EH, Lockett S, Dunlop NM, Wang JM: Activation of Toll-like receptor 2 on microglia promotes cell uptake of Alzheimer disease-associated amyloid β peptide. J Biol Chem 2006, 281:3651–3659
13. Liu Y, Walter S, Stagi M, Cherny D, Letiembre M, Schulz-Schaeffer W, Heine H, Penke B, Neumann H, Fassbender K: LPS receptor (CD14): a receptor for phagocytosis of Alzheimer's amyloid peptide. Brain 2005, 128:1778–1789
14. Xie Z, Wei M, Morgan TE, Fabrizio P, Han D, Finch CE, Longo VD: Peroxynitrite mediates neurotoxicity of amyloid β-peptide1-42- and lipopolysaccharide-activated microglia. J Neurosci 2002, 22:3484–3492
15. Takeuchi H, Jin S, Wang J, Zhang G, Kawanokuchi J, Kuno R, Sonobe Y, Mizuno T, Suzumura A: Tumor necrosis factor-α induces neurotoxicity via glutamate release from hemichannels of activated microglia in an autocrine manner. J Biol Chem 2006, 281:21362–21368
16. Suzumura A, Mezitis SG, Gonatas NK, Silberberg DH: MHC antigen expression on bulk isolated macrophage-microglia from newborn mouse brain: induction of Ia antigen expression by γ-interferon. J Neuroimmunol 1987, 15:263–278
17. Naiki H, Nakakuki K: First-order kinetic model of Alzheimer's β-amyloid fibril extension in vitro. Lab Invest 1996, 74:374–383
18. Dahlgren KN, Manelli AM, Stine WB Jr, Baker LK, Krafft GA, LaDu MJ: Oligomeric and fibrillar species of amyloid-β peptides differentially affect neuronal viability. J Biol Chem 2002, 277:32046–32053
19. Pollock JS, Forstermann U, Mitchell JA, Warne TD, Schmidt HHHW, Nakane M, Murad F: Purification and characterization of particulate endothelium-derived relaxing factor synthase from cultured and native bovine aortic endothelial cells. Proc Natl Acad Sci USA 1991, 88:10480–10484
20. Takeuchi H, Mizuno T, Zhang G, Wang J, Kawanokuchi J, Kuno R, Suzumura A: Neuritic beading induced by activated microglia is an early feature of neuronal dysfunction toward neuronal death by inhibition of mitochondrial respiration and axonal transport. J Biol Chem 2005, 280:10444–10454
21. Lesné S, Koh MT, Kotilinek L, Kayed R, Glabe CG, Yang A, Gallagher M, Ashe KH: A specific amyloid-β protein assembly in the brain impairs memory. Nature 2006, 440:352–357
22. Maurice T, Lockhart BP, Privat A: Amnesia induced in mice by centrally administered β-amyloid peptides involves cholinergic dysfunction. Brain Res 1996, 706:181–193
23. Alkam T, Nitta A, Mizoguchi H, Itoh A, Nabeshima T: A natural scavenger of peroxynitrites, rosmarinic acid, protects against impairment of memory induced by Aβ (25-35). Behav Brain Res 2007, 180:139–145
24. Kamei H, Nagai T, Nakano H, Togan Y, Takayanagi M, Takahashi K, Kobayashi K, Yoshida S, Maeda K, Takuma K, Nabeshima T, Yamada K: Repeated methamphetamine treatment impairs recognition memory through a failure of novelty-induced ERK1/2 activation in the prefrontal cortex of mice. Biol Psychiatry 2006, 59:75–84
25. Mizoguchi H, Takuma K, Fukakusa A, Ito Y, Nakatani A, Ibi D, Kim HC, Yamada K: Improvement by minocycline of methamphetamine-induced impairment of recognition memory in mice. Psychopharmacology 2008, 196:233–241
26. Mouri A, Noda Y, Hara H, Mizoguchi H, Tabira T, Nabeshima T: Oral vaccination with a viral vector containing Aβ cDNA attenuates age-related Aβ accumulation and memory deficits without causing inflammation in a mouse Alzheimer model. FASEB J 2007, 21:2135–2148
27. Franklin KBJ, Paxinos G: The mouse brain: in stereotaxic coordinates. San Diego, Academic 1997, pp. 69–89
28. Scholtzova H, Kascsak RJ, Bates KA, Boutajangout A, Kerr DJ, Meeker HC, Mehta PD, Spinner DS, Wisniewski T: Induction of Toll-like receptor 9 signaling as a method for ameliorating Alzheimer's disease-related pathology. J Neurosci 2009, 29:1846–1854
29. Lee TS, Chau LY: Heme oxygenase-1 mediates the anti-inflammatory effect of interleukin-10 in mice. Nat Med 2002, 8:240–246
30. Krug A, Rothenfusser S, Hornung V, Jahrsdorfer B, Blackwell S, Ballas ZK, Endres S, Krieg AM, Hartmann G: Identification of CpG oligonucleotide sequences with high induction of IFN-α/β in plasmacytoid dendritic cells. Eur J Immunol 2001, 31:2154–2163
31. Selkoe DJ: Alzheimer's disease is a synaptic failure. Science 2002, 298:789–791
32. Demuro A, Mina E, Kayed R, Milton SC, Parker I, Glabe CG: Calcium dysregulation and membrane disruption as a ubiquitous neurotoxic mechanism of soluble amyloid oligomers. J Biol Chem 2005, 280:17294–17300
33. Shankar GM, Bloodgood BL, Townsend M, Walsh DM, Selkoe DJ, Sabatini BL: Natural oligomers of the Alzheimer amyloid-β protein induce reversible synapse loss by modulating an NMDA-type glutamate receptor-dependent signaling pathway. J Neurosci 2007, 27:2866–2875
34. Knobloch M, Farinelli M, Konietzko U, Nitsch RM, Mansuy IM: Aβ oligomer-mediated long-term potentiation impairment involves protein phosphatase 1-dependent mechanisms. J Neurosci 2007, 27:7648–7653
35. Townsend M, Mehta T, Selkoe DJ: Soluble Aβ inhibits specific signal transduction cascades common to the insulin receptor pathway. J Biol Chem 2007, 282:33305–33312
36. Manelli AM, Bulfinch LC, Sullivan PM, LaDu MJ: Aβ42 neurotoxicity in primary co-cultures: effect of apoE isoform and Abeta conformation. Neurobiol Aging 2007, 28:1139–1147
37. Lue LF, Walker DG, Rogers J: Modeling microglial activation in Alzheimer's disease with human postmortem microglial cultures. Neurobiol Aging 2001, 22945–956
38. Combs CK, Karlo JC, Kao SC, Landreth GE: β-Amyloid stimulation of microglia and monocytes results in TNF α-dependent expression of inducible nitric oxide synthase and neuronal apoptosis. J Neurosci 2001, 21:1179–1188
39. Tahara K, Kim HD, Jin JJ, Maxwell JA, Li L, Fukuchi K: Role of Toll-like receptor signalling in Aβ uptake and clearance. Brain 2006, 129: 3006–3019
40. Maines MD: The heme oxygenase system: a regulator of second messenger gases. Annu Rev Pharmacol Toxicol 1997, 37:517–554
41. Atamna H, Frey WH II: A role for heme in Alzheimer's disease: heme binds amyloid β and has altered metabolism. Proc Natl Acad Sci USA 2004, 101:11153–11158
42. Takahashi M, Doré S, Ferris CD, Tomita T, Sawa A, Wolosker H, Borchelt DR, Iwatsubo T, Kim SH, Thinakaran G, Sisodia SS, Snyder SH: Amyloid precursor proteins inhibit heme oxygenase activity and augment neurotoxicity in Alzheimer's disease. Neuron 2000, 28:461–473
43. Lee HY, Kim MK, Park KS, Bae YH, Yun J, Park JI, Kwak JY, Bae YS: Serum amyloid A stimulates matrix-metalloproteinase-9 up-regulation via formyl peptide receptor like-1-mediated signaling in human monocytic cells. Biochem Biophys Res Commun 2005, 330:989–998
44. Dalpke AH, Schäfer MK, Frey M, Zimmermann S, Tebbe J, Weihe E, Heeg K: Immunostimulatory CpG-DNA activates murine microglia. J Immunol 2002, 168:4854–4863
45. Iliev AI, Stringaris AK, Nau R, Neumann H: Neuronal injury mediated via stimulation of microglial Toll-like receptor-9 (TLR9). FASEB J 2004, 18:412–414
46. Krieg AM: Therapeutic potential of Toll-like receptor 9 activation. Nat Rev Drug Discov 2006, 5:471–484
47. Meyer-Luehmann M, Spires-Jones TL, Prada C, Garcia-Alloza M: de Calignon A. Rozkalne A, Koenigsknecht-Talboo J, Holtzman DM, Bacskai BJ, Hyman BT: Rapid appearance and local toxicity of amyloid-β plaques in a mouse model of Alzheimer's disease. Nature 2008, 451:720–724
48. Mandrekar S, Jiang Q, Lee CY, Koenigsknecht-Talboo J, Holtzman DM, Landreth GE: Microglia mediate the clearance of soluble Aβ through fluid phase macropinocytosis. J Neurosci 2009, 29:4252–4262
49. Wu HJ, Sawaya H, Binstadt B, Brickelmaier M, Blasius A, Gorelik L, Mahmood U, Weissleder R, Carulli J, Benoist C, Mathis D: Inflammatory arthritis can be reined in by CpG-induced DC-NK cell cross-talk. J Exp Med 2007, 204:1911–1922
50. Stevens SL, Ciesielski TM, Marsh BJ, Yang T, Homen DS, Boule JL, Lessov NS, Simon RP, Stenzel-Poore MP: Toll-like receptor 9: a new target of ischemic preconditioning in the brain. J Cereb Blood Flow Metab 2008, 28:1040–1047

the FEBS Journal

An E3 ubiquitin ligase, Synoviolin, is involved in the degradation of immature nicastrin, and regulates the production of amyloid β-protein

Tomoji Maeda[1], Toshihiro Marutani[2,*], Kun Zou[1], Wataru Araki[3], Chiaki Tanabe[1], Naoko Yagishita[4], Yoshihisa Yamano[4], Tetsuya Amano[4], Makoto Michikawa[2], Toshihiro Nakajima[4,5,6] and Hiroto Komano[1]

1 Department of Neuroscience, School of Pharmacy, Iwate Medical University, Morioka, Japan
2 Department of Alzheimer's Disease Research, National Center for Geriatrics and Gerontology, Aichi, Japan
3 Department of Demyelinating Disease and Aging, National Institute of Neuroscience, Tokyo, Japan
4 Institute of Medical Science, St. Marianna University School of Medicine, Kawasaki, Japan
5 Choju Medical Institute and Fukushimura Hospital, Toyohashi, Japan
6 Misato Marine Hospital, Kochi, Japan

Keywords
amyloid β-protein; E3 ubiquitin ligase; nicastrin; presenilin; γ-secretase

Correspondence
H. Komano, Department of Neuroscience, School of Pharmacy, Iwate Medical University, 2-1-1 Nishitokuta, Yahaba, Shiwa, Iwate 028-3694, Japan
Fax: +81 19 698 1864
Tel: +81 19 651 5111, extn 5210
E-mail: hkomano@iwate-med.ac.jp

***Present address**
Department of Biology, Faculty of Sciences, Kyushu University Graduate School, Fukuoka, Japan

(Received 13 January 2009, revised 2 August 2009, accepted 6 August 2009)

doi:10.1111/j.1742-4658.2009.07264.x

The presenilin complex, consisting of presenilin, nicastrin, anterior pharynx defective-1 and presenilin enhancer-2, constitutes γ-secretase, which is required for the generation of amyloid β-protein. In this article, we show that Synoviolin (also called Hrd1), which is an E3 ubiquitin ligase implicated in endoplasmic reticulum-associated degradation, is involved in the degradation of endogenous immature nicastrin, and affects amyloid β-protein generation. It was found that the level of immature nicastrin was dramatically increased in *synoviolin*-null cells as a result of the inhibition of degradation, but the accumulation of endogenous presenilin, anterior pharynx defective-1 and presenilin enhancer-2 was not changed. This was abolished by the transfection of exogenous Synoviolin. Moreover, nicastrin was co-immunoprecipitated with Synoviolin, strongly suggesting that nicastrin is the substrate of Synoviolin. Interestingly, amyloid β-protein generation was increased by the overexpression of Synoviolin, although the nicastrin level was decreased. Thus, Synoviolin-mediated ubiquitination is involved in the degradation of immature nicastrin, and probably regulates amyloid β-protein generation.

Structured digital abstract
- MINT-7255352: *Synoviolin* (uniprotkb:Q9DBY1) *physically interacts* (MI:0915) with *NCT* (uniprotkb:P57716) by *anti tag coimmunoprecipitation* (MI:0007)
- MINT-7255377: *Ubiquitin* (uniprotkb:P62991) *physically interacts* (MI:0915) with *NCT* (uniprotkb:P57716) by *anti bait coimmunoprecipitation* (MI:0006)
- MINT-7255363: *NCT* (uniprotkb:P57716) *physically interacts* (MI:0915) with *Synoviolin* (uniprotkb:Q9DBY1) by *anti bait coimmunoprecipitation* (MI:0006)

Introduction

Amyloid β-protein (Aβ), which is the major component of senile plaques in the brains of patients with Alzheimer's disease, is generated from the amyloid precursor protein (APP) through its sequential proteolytic

Abbreviations
Aβ, amyloid β-protein; APH-1, anterior pharynx defective-1; APP, β-amyloid precursor protein; CTF, C-terminal fragment; ER, endoplasmic reticulum; NCT, nicastrin; NTF, N-terminal fragment; PEN-2, presenilin enhancer-2; PS, presenilin.

cleavage catalyzed by β- and γ-secretases [1]. β-Secretase has been identified as a membrane-tethered aspartyl protease [2]. γ-Secretase activity is attributed to the presenilin (PS) complex, which is composed of four transmembrane proteins: PS, nicastrin (NCT), presenilin enhancer-2 (PEN-2) and anterior pharynx defective-1 (APH-1) (collectively named PS cofactors in this study) (reviewed in [3]). Full-length PS is endoproteolytically processed into two fragments: the N-terminal fragment (NTF) and the C-terminal fragment (CTF) [4]. The processed PS resides in the γ-secretase complex (reviewed in [3]). Endogenous PS, NCT, PEN-2 and APH-1 are mainly localized in the endoplasmic reticulum (ER) and Golgi [5], and the properly assembled complex is transported through the secretory pathway to localize predominantly in the Golgi and then at the cell surface [6,7].

NCT is a type I transmembrane protein that possesses many potential glycosylation sites within its large ectodomain [8]. Several studies have established that three principal forms of NCT exist in cells: the unglycosylated, nascent protein (~ 80 kDa); an immature N-linked glycosylated species (immature NCT, ~ 110 kDa); and a mature N-linked isoform (mature NCT, ~ 150 kDa) which is formed after entering the Golgi apparatus [9]. The mature NCT associates with active γ-secretase [10] and, importantly, PS is required for the full post-translational generation of this mature NCT species [9]. In addition, NCT is critical for the stability and trafficking of other γ-secretase components, and NCT affects Aβ production [11].

Interestingly, the cellular level of PS is tightly limited [12]. Excess PS cofactors which fail to reside in the complex, such as full-length PS, mostly undergo ubiquitin/proteasome-mediated degradation, although the precise mechanism of elimination of excess cofactors is not fully understood [12].

Ubiquitination is required for proteasome-mediated degradation, although, recently, accumulating evidence has shown that ubiquitin has multiple functions, including intracellular trafficking (reviewed in [13]), which is accomplished through the sequential actions of enzymes: an activating enzyme (E1), a conjugating enzyme (E2) and a ligase (E3) (reviewed in [14]). Of the three enzymes, E3 enzymes are the key determining factors in substrate protein selection. Synoviolin, a representative of ER-resident E3 ubiquitin ligase, is a mammalian homolog of yeast Hrd1 [15]. Synoviolin is also a pathogenic factor in rheumatoid arthritis [16], and is involved in ER-associated degradation [17]. The substrates of Synoviolin were found to include polyglutamine-expanded huntingtin [18], the tumor suppressor gene p53 [19] and Parkin-associated endothelin receptor-like receptor [20].

In this study, we addressed whether Synoviolin is involved in the degradation of PS cofactors using *synoviolin*-null cells, as PS cofactors undergo the ubiquitin/proteasome pathway. We report that Synoviolin is involved in the degradation of immature NCT and regulates Aβ generation.

Results

Accumulation of immature NCT in *synoviolin*-null cells

To investigate whether Synoviolin is involved in the degradation of PS cofactors, we first compared the levels of PS cofactors by immunoblotting between *synoviolin*-null cells and wild-type (wt) cells. As shown in Fig. 1, the level of endogenous immature NCT was found to be markedly increased in *synoviolin*-null cells, compared with wt cells, although endogenous PS, APH-1 and PEN-2 were not changed in *synoviolin*-null cells. Interestingly, the mobilities of immature and mature NCT on the gel in *synoviolin*-null cells were slightly faster than that in wt cells (Fig. 1A). This is probably a result of the difference in the degree of sugar modification, because deglycosylation treatment of NCT in *synoviolin*-null cells resulted in a similar mobility to that in wt cells (Fig. S1, see Supporting Information). We also determined the levels of γ-secretase-unrelated ER protein (calnexin) and cytoskeleton protein (tubulin) in these cells as the internal control proteins. The calnexin and tubulin levels were found to be similar between these cells, confirming that the same amount of protein was loaded in each lane (Fig. 1A). In addition, the observed accumulation of endogenous immature NCT in *synoviolin*-null cells was abolished by exogenously expressed Synoviolin, but not by the expression of Synoviolin C307A mutant lacking E3 ubiquitin ligase activity [21], indicating that the lack of E3 ubiquitin ligase activity of Synoviolin causes the accumulation of immature NCT (Fig. 1B, right panel). As shown in Fig. 1B (left panel), the overexpression of Synoviolin in wt cells decreased both immature and mature NCT levels; however, very interestingly, the expression of Synoviolin C307A mutant in wt cells caused the accumulation of much more immature NCT than mature NCT. Because the C307A mutant inhibits the ubiquitination mediated by endogenous Synoviolin in a dominant-negative manner, as reported previously [21], this result strongly suggests that Synoviolin-mediated ubiquitination is involved in the preferential degradation of immature NCT.

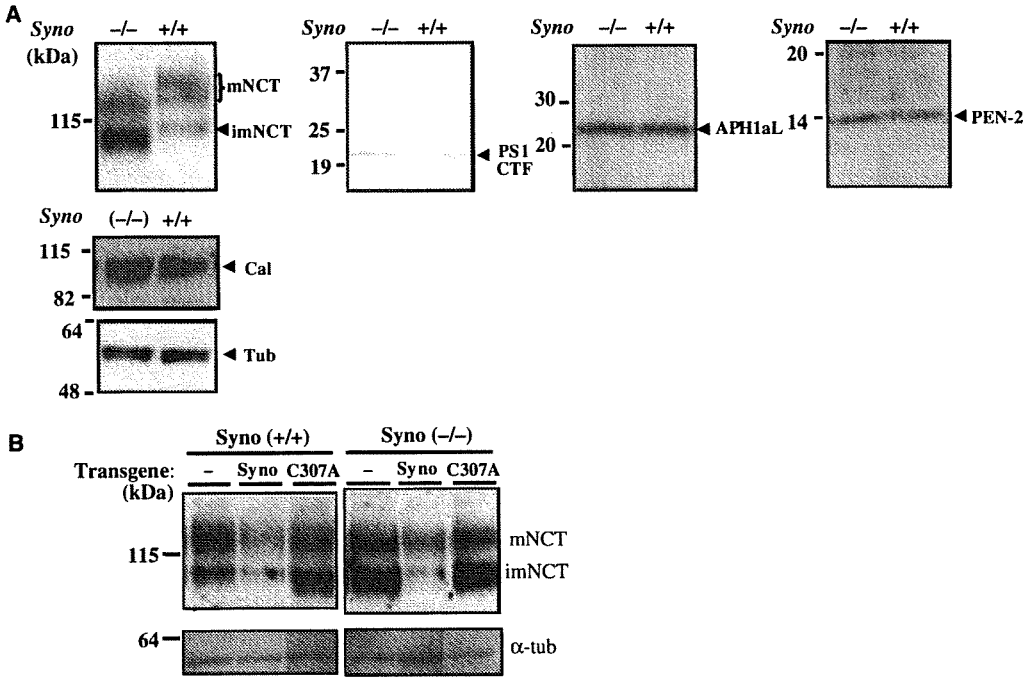

Fig. 1. Accumulation of immature NCT in *synoviolin*-null fibroblasts. (A) The components of the PS complex (NCT, PS-1, APH-1, PEN-2) in the lysate (20 μg) of *synoviolin*-null fibroblasts were detected by immunoblotting with anti-NCT IgG, anti-APH1aL IgG and anti-PEN-2 IgG. Calnexin and α-tubulin in the lysate were also immunodetected as internal markers. −/−, *synoviolin*-null fibroblasts; +/+, wt fibroblasts. (B) NCT in the lysates from wt fibroblasts (left panel) and *synoviolin*-null fibroblasts (right panel), retrovirally expressing Synoviolin or Synoviolin C307A mutant lacking E3 ubiquitin ligase activity, was detected by immunoblotting with anti-NCT IgG. Mutation of the conserved cysteine 307 to alanine in Synoviolin disrupts its ligase activity and this C307A mutant functions in a dominant-negative manner [21]. α-Tubulin in the lysate was also detected as internal marker. imNCT, immature NCT; mNCT, mature NCT; −, mock transfection; Syno, Synoviolin; C307A, Synoviolin C307A mutant; α-tub, α-tubulin.

Effect of Synoviolin on the stability of NCT

Because Synoviolin is an E3 ubiquitin ligase for proteasome-dependent protein degradation, it is most likely that the accumulation of NCT in *synoviolin*-null cells is a result of the suppression of the degradation of NCT. To further investigate this, we next compared the degradation of NCT with time between *synoviolin*-null cells and wt cells. As shown in Fig. 2, western blot analysis of the intracellular degradation of NCT in *synoviolin*-null cells and wt cells following cycloheximide treatment revealed that immature NCT in *synoviolin*-null cells remained stable, as did mature NCT, although, in wt cells, the immature NCT level was preferentially decreased at 10 h after treatment. As a decrease in the immature NCT level seems to include effects of both its maturation and degradation, we further confirmed the degradation of immature NCT in wt cells with treatment by the proteasome inhibitor MG-132. As shown in Fig. 2C, the treatment of wt cells with MG-132 was found to preferentially increase the level of immature NCT compared with that of mature NCT, strongly suggesting that immature NCT is preferentially degraded by the proteasome. Taken together, Synoviolin is most likely to be involved in the preferential degradation of immature NCT via the ubiquitin/proteasome pathway.

Synoviolin interacts with NCT

E3 ligases for ubiquitination confer specificity to the ubiquitin system by directly interacting with the substrate proteins and helping to transfer ubiquitin to them. Therefore, to determine whether NCT is the substrate of Synoviolin, we determined whether Synoviolin interacts with NCT. As shown in Fig. 3, immature NCT was coimmunoprecipitated with anti-FLAG IgG and, in addition, Synovolin was coimmunoprecipitated with anti-NCT IgG when FLAG-tagged Synoviolin and NCT were coexpressed in *synoviolin*-null cells. These results indicate that Synoviolin interacts

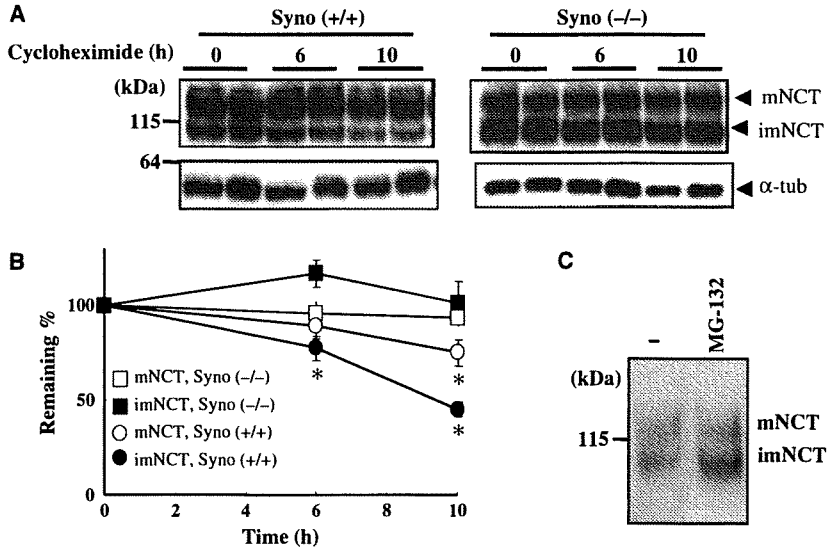

Fig. 2. Degradation of NCT in *synoviolin*-null and wt fibroblasts. (A) *synoviolin*-null and wt fibroblasts were treated with 20 μg·mL^{-1} cycloheximide and harvested at the times indicated. NCT in RIPA-solubilized lysates (10 μg) was detected by immunoblotting with anti-NCT antibody. α-Tubulin in the lysates was also immunodetected as an internal control for a stable protein. Each sample was duplicated. imNCT, immature NCT; mNCT, mature NCT; α-Tub, α-tubulin. (B) The intensities of the bands corresponding to immature NCT and mature NCT in (A) were densitometrically quantified using a luminescent image analyzer LAS-3000 (Fuji Photo Film Co., Ltd., Tokyo, Japan). NCT levels remaining at each time point were calculated as a percentage of the intensity at time zero. Each value is the average of four independent experiments. Asterisk indicates significant differences from time zero [significant difference at $P < 0.05$ (Student's *t*-test)]. (C) Wt fibroblasts were treated with 10 μM MG-132 for 10 h, and NCT in the RIPA-solubilized lysates (10 μg) was detected by immunoblotting with anti-NCT antibody. –, cells treated without MG-132.

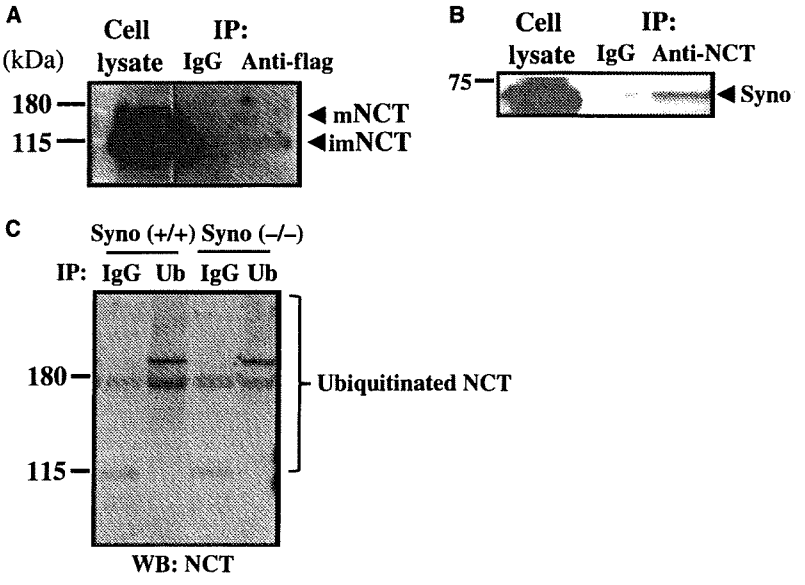

Fig. 3. Synoviolin interacts with NCT. (A) The cell lysates of *synoviolin*-null fibroblasts transiently coexpressing FLAG-tagged Synoviolin and NCT were immunoprecipitated with anti-FLAG antibody and immunodetected with anti-NCT antibody. (B) The same cell lysates were immunoprecipitated with anti-NCT antibody and then immunodetected with anti-Synoviolin antibody. (C) After *synoviolin*-null and wt fibroblasts transiently transfected with NCT had been treated with cycloheximide and lactacystin for 8 h, the cells were harvested. The RIPA-solubilized lysates (1 mg) were immunoprecipitated with anti-ubiquitin mouse antibody (mouse IgG for control) and then immunodetected with anti-NCT antibody. IP, immunoprecipitation; WB, western blot.

with immature NCT. In addition, the degree of ubiquitination of NCT in wt cells was also found to be slightly higher than that in *synoviolin*-null cells (Fig. 3C). However, it was also noted that NCT was slightly ubiquitinated even in *synoviolin*-null cells. Therefore, it is most likely that NCT is a substrate of Synoviolin, but the other E3 ubiquitin ligase also appears to ubiquitinate NCT.

Detection of NCT on the cell surface in *synoviolin*-null cells

Only mature NCT goes to the cell surface, and immature NCT stays within the cells, as reported previously [6,22]. As the level of immature NCT was greatly increased and the molecular weight of NCT was changed slightly in *synoviolin*-null cells, we investigated whether the cellular localization of NCT was different between *synoviolin*-null cells and wt cells. To determine this, we detected NCT localized at the plasma membrane in *synoviolin*-null cells. For this purpose, we labeled the cell surface proteins with biotin, and then detected the surface-biotinylated NCT by immunoblotting with anti-NCT IgG. As shown in Fig. 4A, we found that both immature and mature NCT were clearly detected on the cell surface in *synoviolin*-null cells, although, in wt cells, only mature NCT was detected on the cell surface. In addition, the mature NCT level on the cell surface was increased in *synoviolin*-null cells (Fig. 4B) [percentage of mature NCT at the cell surface relative to that in the total lysate: 24% (wt) versus 64% (Syn−/−)]. These results indicate that a functional deletion of Synoviolin causes a change in the intracellular trafficking of NCT.

Effect of Synoviolin on the production of Aβ

NCT is one of the essential cofactors of the γ-secretase complex. We therefore investigated the effect of the Synoviolin-mediated degradation of NCT on Aβ generation. In Fig. 5, we measured the Aβ level secreted from wt fibroblasts overexpressing APP [23]. As shown in Fig. 5A, B, the overexpression of Synoviolin enhanced the production of Aβ40 and Aβ42 by about twofold, whereas the secretion of soluble APP was not changed in these cells. Figure 5C also showed that the endogenous NCT level was decreased and the intracellular APP level was not changed by the overexpression of Synoviolin. Previously, the targeting of NCT to the cell surface enhanced Aβ generation, because one of the main Aβ generation sites is likely to be in the cell surface [6]. Therefore, it is possible that the overexpression of Synoviolin enhances the localization of NCT at the cell surface, resulting in an enhancement of Aβ generation. To test this possibility, we measured the level of NCT on the cell membrane. No increase in the cell surface NCT level in cells overexpressing Synoviolin was observed (Fig. 5D).

Discussion

In this study, we showed that Synoviolin is involved in the intracellular degradation of NCT. Of the four

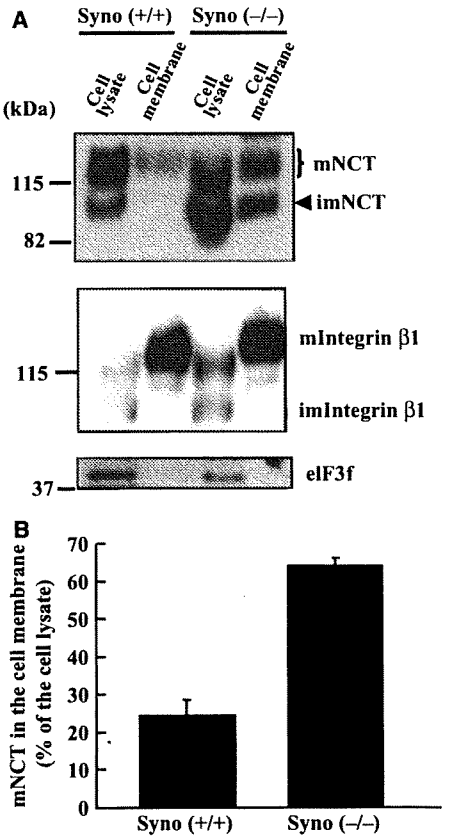

Fig. 4. Cell surface distribution of immature and mature NCT in *synoviolin*-null fibroblasts. (A) Cell surface proteins of *synoviolin*-null and wt fibroblasts were biotinylated as described in Materials and methods. The lysates of surface-biotinylated cells were then incubated with streptavidin–agarose. Total lysate (20 μg) and biotinylated proteins (streptavidin–agarose bound) were immunodetected with anti-NCT IgG, anti-integrin β1 IgG (as a control for the cell surface protein) [22] and anti-eIF3f IgG (as a control for the cytosolic protein) [32]. imNCT, immature NCT; mNCT, mature NCT; m integrin β1, mature integrin β1; im integrin β1, immature integrin β1. (B) Band intensities were densitometrically quantified with a luminescent image analyzer LAS-3000 (Fuji Photo Film Co., Ltd.), and the percentage mature NCT level in the cell membrane relative to that in the total cell lysate was calculated. Data are the average of two independent experiments. The percentage immature NCT level in the cell membrane relative to that in the total cell lysate in *synoviolin*-null cells was 22.0 ± 4.5%.

γ-secretase components, only NCT was found to be degraded by Synoviolin. In addition, Synoviolin appears to preferentially target immature NCT for degradation, because *synoviolin*-null cells exhibited the accumulation of immature NCT, and the expression of the dominant-negative Synoviolin mutant lacking E3 ubiquitin ligase activity in wt cells caused a greater accumulation of immature NCT than mature NCT.

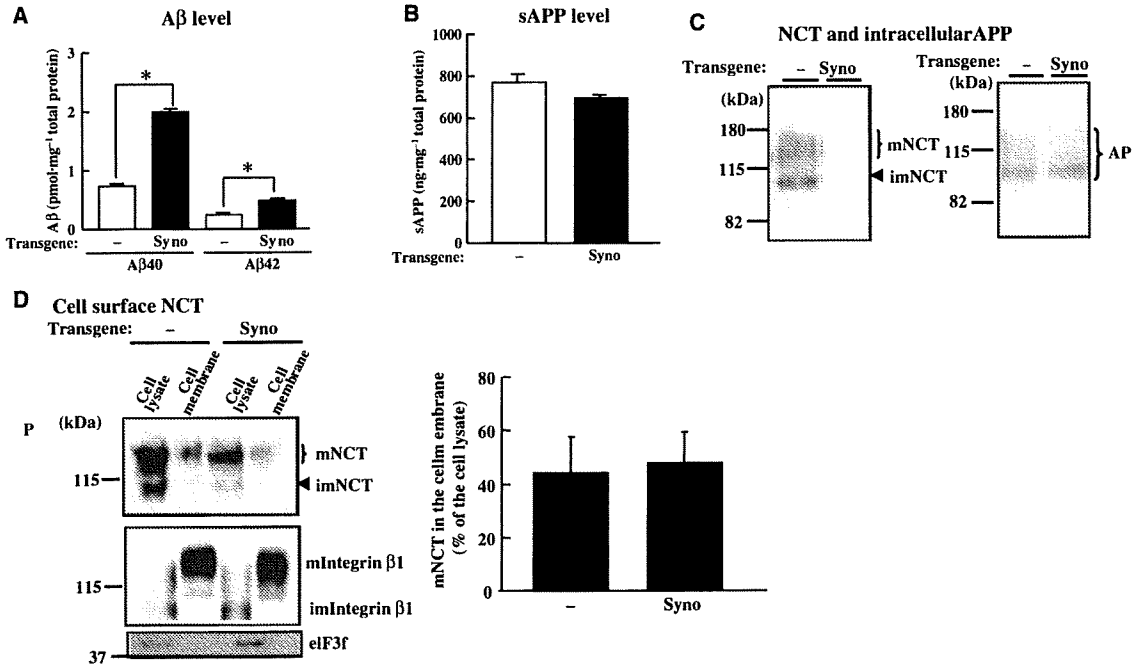

Fig. 5. Effect of the overexpression of Synoviolin on Aβ generation. Wild-type murine fibroblasts expressing APP were retrovirally expressed with Synoviolin. Aβ (A) and soluble APP (B) secreted from the cells during a 96-h culture were detected by ELISA. Values are the means ± SEM of four independent dishes ($n = 4$). Asterisk indicates significant differences from mock [significant difference at $P < 0.01$ (Student's *t*-test)]. (C) NCT and intracellular APP in the cell lysates were immunodetected with anti-NCT IgG and 22C11 respectively. (D) Left panel: cell surface NCT in the mock- or Synovilin-transfected cells was immunodetected as described in Fig. 3. Integrin β1 (as a control for the cell surface protein) and eIF3f (as a control for the cytosolic protein) were also immunodetected. Similar results were obtained from three independent experiments. m integrin β1, mature integrin β1; im integrin β1, immature integrin β1. Right panel: the band intensities were quantified, and the percentage mature NCT level in the cell membrane relative to that of the total cell lysate is shown. Data are the average of three independent experiments. –, mock transfection; Syno, Synoviolin transfection; imNCT, immature NCT; mNCT, mature NCT.

Interestingly, the sugar modification of NCT in *synoviolin*-null cells appeared to be slightly different from that in wt cells. This may suggest that Synovilin-mediated ubiquitination also regulates the trafficking of NCT within the Golgi compartment, because the maturation of the sugar modification of the protein occurs within the Golgi compartment. Recently, there has been an expansion of the recognized roles for ubiquitin in processes other than proteasome-dependent proteolysis, which includes intracellular trafficking (reviewed in [13]). In this regard, it is noteworthy that both immature NCT and mature NCT delivered to the cell surface were increased in *synoviolin*-null cells, although only the mature form of NCT goes to the cell surface in wt cells (Fig. 4). It appears that Synoviolin somehow suppresses the direct delivery of NCT from ER to the cell surface. Previously, it has been shown that Synoviolin increases the membrane localization of huntingtin protein [18], also suggesting that Synoviolin is involved in intracellular trafficking.

We also found that NCT interacts with Synoviolin (Fig. 3), strongly suggesting that NCT is the substrate of Synoviolin. As reported previously, NCT undergoes ubiquitination [24]. We found that the degree of ubiquitination of NCT in wt cells was higher than that in *synoviolin*-null cells. Therefore, NCT is most likely to be a substrate of Synoviolin. However, the other E3 ubiquitin ligase also appears to ubiquitinate NCT, because NCT was ubiqutinated slightly even in *synoviolin*-null cells. Indeed, in *synoviolin*-null cells, NCT started to degrade more than 10 h after cycloheximide treatment (data not shown). Further study of the mechanism underlying NCT degradation mediated by Synoviolin, including an *in vitro* study, is needed.

It was also noted that the overexpression of Synoviolin increased the Aβ level, whereas the cellular level of NCT decreased in transfected cells, because a decreased NCT level would be expected to decrease the Aβ level. Because the levels of full-length APP and soluble APP were not changed (Fig. 5), it is likely that γ-cleavage was increased. As reported previously [25],

the cell membrane NCT level is thought to be more important than the intracellular level of NCT for Aβ generation. Therefore, we investigated whether Synoviolin enhances the cell surface localization of NCT; however, no increase in the cell membrane NCT level in cells transfected with Synoviolin was observed. It has also been shown that the overexpression of SEL-10, that is an E3 ligase for PS1 ubiquitination, causes a decrease in the level of PS1, but an increase in Aβ secretion [26]. This suggests that SEL-10-mediated ubiquitination modulates the PS1 complex in APP processing, although the exact mechanism is not known. Therefore, likewise, Synoviolin-mediated ubiquitination can also regulate Aβ generation, possibly through the modulation of intracellular trafficking. As the overexpression of Synoviolin was suggested to increase γ-cleavage, as mentioned above, the overexpression of Synoviolin, probably through ubiquitination, could promote the trafficking of the PS complex to the site at which γ-cleavage occurs, or activate γ-secretase itself.

In this study, we conclude that Synoviolin is involved in the degradation of immature NCT. We have also shown that the expression of Synoviolin enhances Aβ generation. Further study of the mechanism underlying the enhancement of Aβ generation by Synoviolin will clarify the interaction between the ubiqutination of the PS complex and APP processing.

Materials and methods

Antibodies, reagents and cell lines

A mouse anti-PS1 monoclonal IgG (for the CTF of PS1) was purchased from Chemicon International (Temecula, CA, USA). A rabbit anti-NCT IgG and a mouse NCT monoclonal IgG were purchased from Sigma (St. Louis, MO, USA) and Chemicon International, respectively. MG-132 was purchased from Sigma. A rabbit anti-APH1aL antibody was purchased from COVANCE (Berkeley, CA, USA). Anti-PEN-2 IgM was provided by Dr Thinakaran [27,28]. Anti-α-tubulin and anti-calnexin IgG were purchased from Santa Cruz Biotechnology, Inc. (Santa Cruz, CA, USA). Anti-APP N-terminal antibody 22C11 was purchased from Sigma. Anti-HRD1 (Synoviolin) C-terminal antibody was purchased from ABGENT (San Diego CA, USA). Anti-elF3f was purchased from Rockland Inc. (Gilbertsville, PA, USA). Anti-integrin β1 antibody was purchased from BD Biosciences (San Jose, CA, USA). Monoclonal antibody against mono- and polyubiquitin was purchased from BIOMOL (Plymouth Meeting, PA, USA). Synoviolin-null murine fibroblasts [29] and murine fibroblasts overexpressing human APP were cultured in Dulbecco's modified Eagle's medium (DMEM; Wako Pure Chemical Industries, Ltd., Osaka, Japan) containing 10% fetal bovine serum.

Plasmids and retrovirus-mediated infection

PMX-Synoviolin was generated as described previously [16]. cDNA encoding Synoviolin C307A mutant was generated by overlap PCR using the following primers: 5′-AAATGTGGTTGGCGGGCAGTCTCTTGGC-3′ and 5′-ACTGCCCGCCAACCACATTTTCC-3′. The PCR product was verified by sequencing. The retrovirus-mediated infection was carried out as reported previously [30].

Cycloheximide treatment

Cells (5×10^5) plated on 60 mm tissue culture dishes were grown for 24 h; cycloheximide was then added to a final concentration of 20 $\mu g \cdot mL^{-1}$. At various times after the addition of cycloheximide, the cells were harvested and lysed in RIPA buffer (150 mM NaCl, 10 mM Tris/HCl pH 7.5, 1% Nonidet P-40, 0.1% SDS and 0.2% sodium deoxycholate) containing a protease inhibitor cocktail.

Immunoprecipitation, immunoblotting and ELISA

Cultured cells were lysed in RIPA buffer containing a protease inhibitor cocktail. The solubilized proteins were subjected to immunoprecipitation as described previously [31]. The precipitated proteins were resolved by SDS-PAGE on 4–20% gel for the detection of PS and NCT. Immunoblotting was performed as reported previously [31]. ELISAs for Aβ and soluble APP were performed using a βAmyloid ELISA kit (Wako Pure Chemical Industries, Ltd., Osaka, Japan) and human soluble APP ELISA kit (IBL Co., Ltd., Nagoya, Japan), respectively.

Cell surface biotinylation

Cell surface biotinylation was carried out using a cell surface protein isolation kit (Pierce, Rockford, IL, USA). The cells were grown in four 10 cm tissue culture dishes, and washed twice with ice-cold NaCl/P_i. The cells were incubated in 10 mL of ice-cold sulfosuccinimidy-2-(biotinamido)-ethyl-1,3-dithiopropionate (0.25 $mg \cdot mL^{-1}$) in ice-cold NaCl/P_i for 30 min at 4 °C, and then 500 μL of the quenching solution were added to each dish to quench the reaction. The cells were scraped and washed twice with Tris-buffered saline (TBS) (10 mM Tris/HCl pH 7.5, 150 mM NaCl) and lysed in lysis buffer containing protease inhibitors. Each lysate was incubated with streptavidin–agarose beads at 4 °C for 60 min, and the captured proteins were eluted with 50 mM dithiothreitol in Laemmli's SDS sample buffer.

Acknowledgements

We thank Dr Gopal Thinakaran for providing anti-PEN-2 IgG. This study was supported in part by a grant-in-aid for scientific research from the Ministry of Education, Culture, Sports, Science and Technology of Japan, and by a grant from the Ministry of Health, Labor and Welfare of Japan. We thank Dr Paul Langman for assistance with the English.

References

1 Selkoe DJ (2002) Deciphering the genesis and fate of amyloid β-protein yields novel therapies for Alzheimer disease. *J Clin Invest* **110**, 1375–1381.
2 Vassar R, Bennett BD, Babu-Khan S, Kahn S, Mendiaz EA, Denis P, Teplow DB, Ross S, Amarante P, Loeloff R *et al.* (1999) β-Secretase cleavage of Alzheimer's amyloid precursor protein by the transmembrane aspartic protease BACE. *Science* **286**, 735–741.
3 De Strooper B (2003) Aph-1, Pen-2, and Nicastrin with Presenilin generate an active γ-Secretase complex. *Neuron* **38**, 9–12.
4 Thinakaran G, Borchelt DR, Lee MK, Slunt HH, Spitzer L, Kim G, Ratovitsky T, Davenport F, Nordstedt C, Seeger M *et al.* (1996) Endoproteolysis of presenilin 1 and accumulation of processed derivatives in vivo. *Neuron* **17**, 181–190.
5 Gu Y, Chen F, Sanjo N, Kawarai T, Hasegawa H, Duthie M, Li W, Ruan X, Luthra A, Mount HT *et al.* (2003) APH-1 interacts with mature and immature forms of presenilins and nicastrin and may play a role in maturation of presenilin–nicastrin complexes. *J Biol Chem* **278**, 7374–7380.
6 Kaether C, Lammich S, Edbauer D, Ertl M, Rietdorf J, Capell A, Steiner H & Haass C (2002) Presenilin-1 affects trafficking and processing of βAPP and is targeted in a complex with nicastrin to the plasma membrane. *J Cell Biol* **158**, 551–561.
7 Kim SH, Yin YI, Li YM & Sisodia SS (2004) Evidence that assembly of an active γ-secretase complex occurs in the early compartments of the secretory pathway. *J Biol Chem* **279**, 48615–48619.
8 Yu G, Nishimura M, Arawaka S, Levitan D, Zhang L, Tandon A, Song YQ, Rogaeva E, Chen F, Kawarai T *et al.* (2000) Nicastrin modulates presenilin-mediated notch/glp-1 signal transduction and βAPP processing. *Nature* **407**, 48–54.
9 Leem JY, Vijayan S, Han P, Cai D, Machura M, Lopes KO, Veselits ML, Xu H & Thinakaran G (2002) Presenilin 1 is required for maturation and cell surface accumulation of nicastrin. *J Biol Chem* **277**, 19236–19240.
10 Kimberly WT, LaVoie MJ, Ostaszewski BL, Ye W, Wolfe MS & Selkoe DJ (2002) Complex N-linked glycosylated nicastrin associates with active γ-secretase and undergoes tight cellular regulation. *J Biol Chem* **277**, 35113–35117.
11 Zhang YW, Luo WJ, Wang H, Lin P, Vetrivel KS, Liao F, Li F, Wong PC, Farquhar MG, Thinakaran G *et al.* (2005) Nicastrin is critical for stability and trafficking but not association of other presenilin/γ-secretase components. *J Biol Chem* **280**, 17020–17026.
12 Ratovitski T, Slunt HH, Thinakaran G, Price DL, Sisodia SS & Borchelt DR (1997) Endoproteolytic processing and stabilization of wild-type and mutant presenilin. *J Biol Chem* **272**, 24536–24541.
13 Mukhopadhyay D & Riezman H (2007) Proteasome-independent functions of ubiquitin in endocytosis and signaling. *Science* **315**, 201–205.
14 Pickart CM (2004) Back to the future with ubiquitin. *Cell* **116**, 181–190.
15 Schulze A, Standera S, Buerger E, Kikkert M, van Voorden S, Wiertz E, Koning F, Kloetzel PM & Seeger M (2005) The ubiquitin-domain protein HERP forms a complex with components of the endoplasmic reticulum associated degradation pathway. *J Mol Biol* **354**, 1021–1027.
16 Amano T, Yamasaki S, Yagishita N, Tsuchimochi K, Shin H, Kawahara K, Aratani S, Fujita H, Zhang L, Ikeda R *et al.* (2003) Synoviolin/Hrd1, an E3 ubiquitin ligase, as a novel pathogenic factor for arthropathy. *Genes Dev* **17**, 2436–2449.
17 Christianson JC, Shaler TA, Tyler RE & Kopito RR (2008) OS-9 and GRP94 deliver mutant alpha1-antitrypsin to the Hrd1-SEL1L ubiquitin ligase complex for ERAD. *Nat Cell Biol* **10**, 272–282.
18 Yang H, Zhong X, Ballar P, Luo S, Shen Y, Rubinsztein DC, Monteiro MJ & Fang S (2007) Ubiquitin ligase Hrd1 enhances the degradation and suppresses the toxicity of polyglutamine-expanded huntingtin. *Exp Cell Res* **313**, 538–550.
19 Yamasaki S, Yagishita N, Sasaki T, Nakazawa M, Kato Y, Yamadera T, Bae E, Toriyama S, Ikeda R, Zhang L *et al.* (2007) Cytoplasmic destruction of p53 by the endoplasmic reticulum-resident ubiquitin ligase 'Synoviolin'. *EMBO J* **26**, 113–122.
20 Omura T, Kaneko M, Onoguchi M, Koizumi S, Itami M, Ueyama M, Okuma Y & Nomura Y (2008) Novel functions of ubiquitin ligase HRD1 with transmembrane and proline-rich domains. *J Pharmacol Sci* **106**, 512–519.
21 Gao B, Lee SM, Chen A, Zhang J, Zhang DD, Kannan K, Ortmann RA & Fang D (2008) Synoviolin promotes IRE1 ubiquitination and degradation in synovial fibroblasts from mice with collagen-induced arthritis. *EMBO Rep* **9**, 480–485.
22 Zou K, Hosono T, Nakamura T, Shiraishi H, Maeda T, Komano H, Yanagisawa K & Michikawa M (2008) Novel role of presenilins in maturation and transport of integrin β1. *Biochemistry* **47**, 3370–3378.

23 Sai X, Kokame K, Shiraishi H, Kawamura Y, Miyata T, Yanagisawa K & Komano H (2003) The ubiquitin-like domain of Herp is involved in Herp degradation, but not necessary for its enhancement of amyloid beta-protein generation. *FEBS Lett* **553**, 151–156.
24 He G, Qing H, Tong Y, Cai F, Ishiura S & Song W (2007) Degradation of nicastrin involves both proteasome and lysosome. *J Neurochem* **101**, 982–992.
25 Morais VA, Leight S, Pijak DS, Lee VM & Costa J (2008) Cellular localization of Nicastrin affects amyloid β species production. *FEBS Lett* **582**, 427–433.
26 Li J, Pauley AM, Myers RL, Shuang R, Brashler JR, Yan R, Buhl AE, Ruble C & Gurney ME (2002) SEL-10 interacts with presenilin 1, facilitates its ubiquitination, and alters A-beta peptide production. *J Neurochem* **82**, 1540–1548.
27 Araki W, Takahashi-Sasaki N, Chui DH, Saito S, Takeda K, Shirotani K, Takahashi K, Murayama KS, Kametani F, Shiraishi H *et al.* (2008) A family of membrane proteins associated with presenilin expression and γ-secretase function. *FASEB J* **22**, 819–827.
28 Luo WJ, Wang H, Li H, Kim BS, Shah S, Lee HJ, Thinakaran G, Kim TW, Yu G & Xu H (2003) PEN-2 and APH-1 coordinately regulate proteolytic processing of presenilin 1. *J Biol Chem* **278**, 7850–7854.
29 Yagishita N, Ohneda K, Amano T, Yamasaki S, Sugiura A, Tsuchimochi K, Shin H, Kawahara K, Ohneda O, Ohta T *et al.* (2005) Essential role of synoviolin in embryogenesis. *J Biol Chem* **280**, 7909–7916.
30 Komano H, Shiraishi H, Kawamura Y, Sai X, Suzuki R, Serneels L, Kawaichi M, Kitamura T & Yanagisawa K (2002) A new functional screening system for identification of regulators for the generation of amyloid β-protein. *J Biol Chem* **277**, 39627–39633.
31 Sudoh S, Kawamura Y, Sato S, Wang R, Saido TC, Oyama F, Sakaki Y, Komano H & Yanagisawa K (1998) Presenilin 1 mutations linked to familial Alzheimer's disease increase the intracellular levels of amyloid beta-protein 1–42 and its N-terminally truncated variant(s) which are generated at distinct sites. *J Neurochem* **71**, 1535–1543.
32 Lagirand-Cantaloube J, Offner N, Csibi A, Leibovitch MP, Batonnet-Pichon S, Tintignac LA, Segura CT & Leibovitch SA (2008) The initiation factor eIF3-f is a major target for atrogin1/MAFbx function in skeletal muscle atrophy. *EMBO J* **27**, 1266–1276.

Supporting information

The following supplementary material is available:
Fig. S1. Deglycosylation of NCT.

This supplementary material can be found in the online version of this article.

Please note: As a service to our authors and readers, this journal provides supporting information supplied by the authors. Such materials are peer-reviewed and may be re-organized for online delivery, but are not copy-edited or typeset. Technical support issues arising from supporting information (other than missing files) should be addressed to the authors.

BJ www.biochemj.org

BJ Metabolism

Biochem. J. (2009) 421, 293–299 (Printed in Great Britain) doi:10.1042/BJ20090286

Dynamic aspects of ascorbic acid metabolism in the circulation: analysis by ascorbate oxidase with a prolonged *in vivo* half-life

Emiko KASAHARA*[1], Misato KASHIBA†, Mika JIKUMARU*, Daisuke KURATSUNE*, Kumi ORITA*, Yurika YAMATE*, Kenjiro HARA*, Atsuo SEKIYAMA*, Eisuke F. SATO* and Masayasu INOUE*

*Department of Biochemistry and Molecular Pathology, Osaka City University Medical School, 1-4-3 Asahimachi, Abeno, Osaka 545-8585, Japan, and †School of Bionics, Tokyo University of Technology, 1401-1 Katakura, Hachioji, Tokyo 192-0982, Japan

Because AA (L-ascorbic acid) scavenges various types of free radicals to form MDAA (monodehydroascorbic acid) and DAA (dehydroascorbic acid), its regeneration from the oxidized metabolites is critically important for humans and other animals that lack the ability to synthesize this antioxidant. To study the dynamic aspects of AA metabolism in the circulation, a long acting AOase (ascorbate oxidase) derivative was synthesized by covalently linking PEG [poly(ethylene glycol)] to the enzyme. Fairly low concentrations of the modified enzyme (PEG–AOase) rapidly decreased AA levels in isolated fresh plasma and blood samples with a concomitant increase in their levels of MDAA and DAA. In contrast, relatively high doses of PEG–AOase were required to decrease the circulating plasma AA levels of both normal rats and ODS (osteogenic disorder Shionogi) rats that lack the ability to synthesize AA. Administration of 50 units of PEG–AOase/kg of body weight rapidly decreased AA levels in plasma and the kidney without affecting the levels in other tissues, such as the liver, brain, lung, adrenal grand and skeletal muscles. PEG–AOase slightly, but significantly, decreased glutathione (GSH) levels in the liver without affecting those in other tissues. Suppression of hepatic synthesis of GSH by administration of BSO [L-buthionin-(*S*,*R*)-sulfoximine] enhanced the PEG–AOase-induced decrease in plasma AA levels. These and other results suggest that the circulating AA is reductively regenerated from MDAA extremely rapidly and that hepatic GSH plays important roles in the regeneration of this antioxidant.

Key words: antioxidant, ascorbate oxidase, ascorbic acid, glutathione, oxidative stress.

INTRODUCTION

The reduced form of AA (ascorbic acid) is a naturally occurring antioxidant that scavenges free radicals to generate its oxidized metabolites, MDAA (monodehydroascorbic acid) and DAA (dehydroascorbic acid) [1–4]. Although plasma levels of the circulating AA in mammals are low (~60 μM), they rapidly undergo oxidation to generate MDAA even under physiological conditions [5–7]. Therefore oxidized metabolites of AA should be reductively regenerated from MDAA and DAA particularly in humans and some mammals that lack the ability to synthesize AA [8]. Because AA synthesis in most animals is restricted to the liver [9–11], AA, MDAA and DAA should be metabolized via inter-organ co-operation to maintain steady-state levels of AA in plasma and tissues [7,12]. Concentrations of AA in cells and tissues are higher than those in plasma by ~2 orders of magnitude. In this context, two types of transport systems for AA and DAA have been reported with mammals, one is the SVCT (Na^+-AA cotransport system) [13–17] and the other is the GLUT (glucose transporter), responsible for the facilitated transport of glucose and DAA [18]. When transported into cells, DAA is enzymatically reduced to AA at the expense of either GSH, thioredoxin or NAD(P)H [19–23]. Because AA does not serve as a substrate for GLUT, AA regenerated from DAA inside cells is kept at high concentrations by a metabolic sink mechanism [24]. Thus cellular activities of SVCT, GLUT and reducing enzymes for MDAA and DAA might determine the steady-state levels of AA in plasma and tissues of animals that lack the activity to synthesize AA; however, the dynamic aspects of transport and metabolism of AA and its oxidized metabolites *in vivo* remain to be elucidated.

In the present study we synthesized PEG [poly(ethylene glycol)]-AOase (ascorbate oxidase), an AA oxidase derivative with a prolonged *in vivo* half-life. Intravenously administered PEG–AOase effectively oxidizes plasma AA to MDAA in a dose-dependent manner. The present study describes the effect of PEG–AOase on plasma and tissue levels of AA, MDAA and DAA in control, STZ (streptozotocin)-treated diabetic rats and ODS (osteogenic disorder Shionogi) rats that lack the ability to synthesize AA [25,26]. The results suggest for the first time that the circulating AA is reductively regenerated extremely rapidly by using hepatic GSH.

MATERIALS AND METHODS

Chemicals

GSH and DTNB [5,5′-dithiobis-(2-nitrobenzoic acid)] were purchased from Wako Pure Chemicals. AOase (EC 1.10.3.3) from cucurbita species, AA, glutathione reductase, DTC (diethyldithiocarbamate), DTPA (diethylenetriamine pentaacetic acid) and STZ were purchased from Sigma. Activated PEG (MW = 10000 Da) was obtained from Seikagaku Kogyo. All other reagents used were the highest grade commercially available.

Animals

Male Wistar rats (8–9 weeks old) obtained from SLC (Shizuoka, Japan) were fed laboratory chow and water *ad libitum* and used for experiments without prior fasting. Unless otherwise stated, they were used for the experiments as normal animals. We also

Abbreviations used: AA, ascorbic acid; AOase, ascorbate oxidase; DAA, dehydroascorbic acid; DTC, diethyldithiocarbamate; DTPA, diethylenetriamine pentaacetic acid; ESR, electron spin resonance; GLUT, glucose transporter; MDAA, monodehydroascorbic acid; ODS, osteogenic disorder Shionogi; PEG, poly(ethylene glycol); STZ, streptozotocin; SVCT, Na^+-AA cotransport system; TCA, trichloroacetic acid.

[1] To whom correspondence should be addressed (email kasahara@med.osaka-cu.ac.jp).

used ODS rats, which lack the ability to synthesize AA, and STZ-induced hyperglycaemic rats. To increase glucose levels in plasma, animals were intravenously administered 50 mg of STZ/kg of body weight 5 days prior to the experiments. The blood glucose levels of STZ-treated rats (435.3 ± 41.3 mg/dl) were higher than those of control animals (117.9 ± 23.0 mg/dl). Male ODS rats (6 weeks old) were obtained from Clea (Osaka, Japan) and allowed free access to normal diet and AA-containing water (1 mg/ml) for 2 weeks. The concentration of AA in the chow was 0.02 %. All experiments were performed according to the Guidelines for Laboratory Animal Care Regulation of Osaka City University Medical School and were approved by the Ethical Committee of our University.

Synthesis of PEG–AOase

Lysyl amino groups of AOase were covalently linked with activated PEG as described previously [27]. Briefly, the reaction mixture contained, in a final volume of 1 ml of 50 mM bicarbonate (pH 10), 250 units of AOase, 250 mg of PEG and 50 mM AA. The mixture was incubated at 37 °C for 3 h and then for 16 h at 4 °C. The incubated mixture was dialysed at 4 °C against 3 litres of 20 mM PBS (pH 7.4). The activities of AOase and PEG–AOase were determined by measuring the rate of AA decrease. The reaction was stopped by adding 5 mM DTC, and the remaining AA was determined. One unit of the enzyme was defined as the amount of the enzyme required for the oxidation of 1 μmol of AA per min at 37 °C and pH 7.4.

Oxidation of AA by PEG–AOase

Under light ether anaesthesia, blood samples were obtained from the abdominal artery in heparinized tubes. To the fresh blood samples was added Tris/HCl (pH 7.4) to give a final concentration of 20 mM to maintain their pH. Plasma samples were obtained after centrifugation of the blood at 10000 *g* at 4 °C for 1 min. Blood and plasma samples were incubated with 20 m-units/ml of PEG–AOase at 37 °C in air. After incubation with the enzyme, the blood and plasma samples were collected in 1 mM DTC- and DTPA-containing tubes to stop further oxidation of AA. Blood samples were immediately centrifuged at 10000 *g* for 30 s. Plasma samples thus obtained were analysed for AA, MDAA and DAA.

Under urethane anaesthesia, rats were injected with various doses of PEG–AOase. At the indicated times, blood samples were collected from the left femoral vein in 1 mM DTC- and DTPA-containing tubes and analysed for AA, MDAA and DAA. Some animals were intravenously injected with 1 mmol of BSO/kg of body weight prior to the administration of PEG–AOase.

Analysis of AA and GSH levels

Fresh plasma samples were mixed with an equivolume of 10 % TCA (trichloroacetic acid). The excised tissues were homogenized using a micro homogenizer (Physcotron; Microtec) in 5 vol. of ice-cold 5 % TCA containing 1 mM DTPA. After centrifugation of the samples at 10000 *g* at 4 °C for 10 min, the acid-soluble fractions were used for the analysis of AA, free thiols and glutathione. AA levels were determined by using HPLC equipped with a Shimazu electrochemical detection system [28,29]. DAA levels were calculated by subtraction of AA levels from total levels of AA in the samples. The total AA level was determined using HPLC analysis after reduction of the acid-soluble fractions with 3.3 mM DTT (dithiothreithol) containing 330 mM K_2HPO_4 for 5 min at room temperature (22 °C) as described previously [30]. Total glutathione (GSH + 2 GSSG) and low-molecular-mass thiols were determined using the method of Tietze [31] and Ellman [32] respectively.

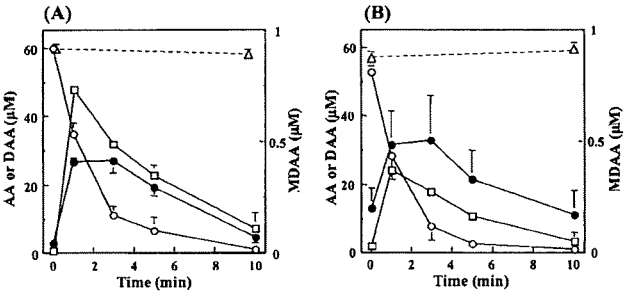

Figure 1 Effect of PEG–AOase on plasma AA levels *in vitro*

Freshly prepared plasma (**A**) or blood (**B**) samples from normal rats were incubated in the presence or absence of 20 m-units of PEG–AOase/ml at 37 °C. At the indicated times, AA (○), MDAA (□) and DAA (●) levels were determined as described in the Materials and methods section. AA levels in the blood and plasma samples remained unchanged after incubation for 10 min in the absence of PEG–AOase (△). Values are means ± S.E.M. ($n = 5$).

ESR (electron spin resonance) analysis

An extracorporeal blood circulation system was established as described previously [33]. Briefly, male Wistar rats were anaesthetized with urethane, and polyethylene tubings (0.60 mm and 0.47 mm in diameter) were inserted into the left femoral artery and vein respectively. The two tubings were connected to an ESR flow cell (200 μl). The flow rate of the blood in the circuit was controlled by a Perista pump at 1 ml/min. Before and after intravenous injection of PEG–AOase, the ESR spectrum of MDAA in the circulation was recorded using a JEOL TES-TE 200 at 37 °C (8 mW of power, 0.079 mT modulation, 334.6 ± 5 mT magnetic field, 5 mT sweep width, 4 min sweep time and a 0.3 s time constant). Concentrations of MDAA were determined by using an external standard based on the signal intensity.

Statistics

Values are expressed as the mean ± S.E.M. derived from 5–15 animals. Statistical analysis was performed using ANOVA followed by a Student's t test and the level of significance was $P < 0.05$.

RESULTS

Oxidation of AA by PEG–AOase in isolated plasma and blood

To elucidate the dynamic aspects of AA metabolism in isolated plasma and blood, the effect of PEG–AOase on the plasma levels of AA and its metabolites were analysed *in vitro*. Incubation with PEG–AOase (20 m-units/ml) rapidly decreased AA levels in plasma with a concomitant increase in MDAA and DAA levels (Figure 1A). Then, the increased MDAA and DAA rapidly decreased at similar rates. When incubated with fresh blood, PEG–AOase also decreased plasma levels of AA and increased MDAA and DAA (Figure 1B). The rate of MDAA increase in blood samples was slightly lower than that observed in the experiment with plasma samples. Under identical conditions, the levels of AA in the plasma (59.9 ± 0.88 μM) and blood (57.1 ± 1.50 μM) remained unchanged (57.9 ± 0.64 μM and 60.5 ± 1.65 μM respectively) at least for 10 min in the absence of PEG–AOase.

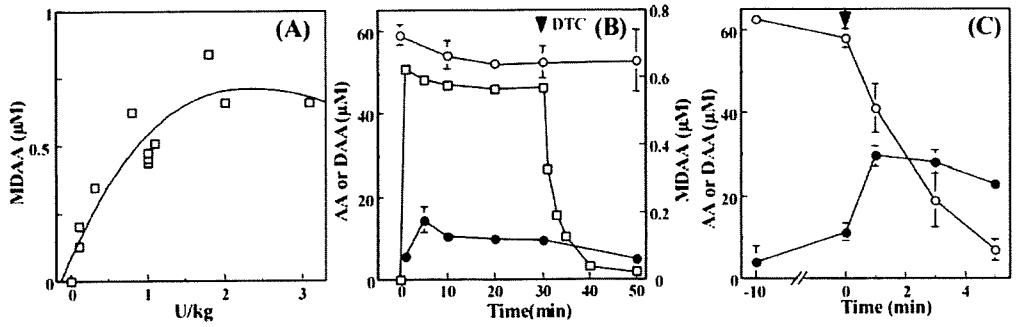

Figure 2 Effect of PEG–AOase on the concentration of AA and its metabolites in the circulation

At 1 min after intravenous administration of various doses of PEG–AOase to normal rats, the levels of the circulating MDAA (□) were determined using the ESR method (**A**) as described in the Materials and methods section. Time-dependent changes in AA (○), MDAA (□) and DAA (●) levels were also measured after administration of 1 unit of PEG–AOase/kg of body weight (**B**). At the indicated time (arrow), the catalytic activity of PEG–AOase was blocked by intravenous administration of 0.1 mmol of DTC/kg of body weight. After 10 min of administration of 1 unit of the enzyme/kg of body weight, blood samples were collected and incubated for 1, 3 and 5 min at 37 °C in air (**C**). Then, plasma levels of AA and DAA were also determined. Values are the means ± S.E.M. ($n = 8 \sim 15$).

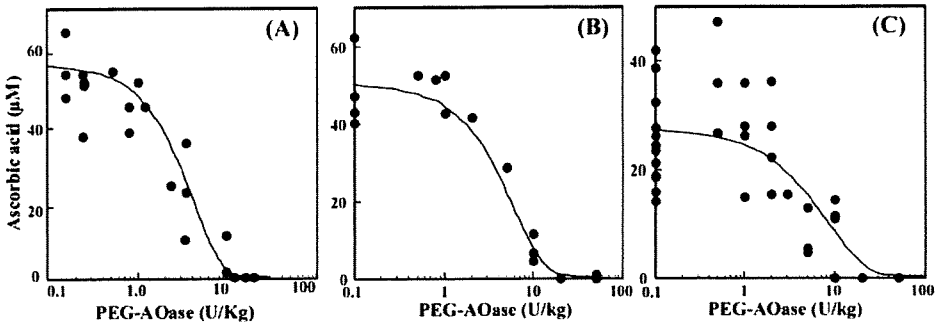

Figure 3 Effect of PEG–AOase on the circulating AA

Various doses of PEG–AOase were injected intravenously into normal (**A**), ODS (**B**) and STZ-treated (**C**) rats. Plasma AA levels in the circulation were determined 2 h after the administration. Other conditions were as in Figure 2. Values are means ± S.E.M. ($n = 5 \sim 11$).

Oxidation of AA by PEG–AOase in the circulation

To elucidate the dynamic aspects of the metabolism and transport of AA in the circulation, the effect of PEG–AOase on the circulating plasma levels of AA and its metabolites were analysed *in vivo* using the ESR blood circulation system as described in the Material and methods section. Intravenous administration of PEG–AOase increased plasma levels of MDAA in a dose-dependent manner (Figure 2A). Figure 2(B) shows the time-dependent changes in AA and its oxidized metabolites in plasma after administration of PEG–AOase. Although PEG–AOase (1 unit/kg of body weight) rapidly increased plasma levels of MDAA in the circulation, no significant decrease was found to occur with circulating AA levels (Figure 2B). The increased MDAA in the circulation rapidly decreased after administration of DTC, a chelating agent for Cu^{2+} to inactivate PEG–AOase, suggesting that PEG–AOase continuously oxidized AA while the generated MDAA rapidly disappeared from the circulation.

Although a fairly high dose (1 unit/kg of body weight) of the enzyme failed to decrease AA levels in the circulation, its plasma levels rapidly decreased after isolation of the blood with a concomitant increase in DAA levels as observed with *in vitro* experiments (Figure 2C). Thus we tested the effect of high doses of the enzyme on AA levels in the circulation (Figure 3). PEG–AOase started to decrease the plasma AA levels in normal rats at doses higher than 2 units/kg of body weight (Figure 3A). At PEG–AOase doses higher than 10 units/kg of body weight, AA levels in the circulation rapidly decreased.

Effects of AA synthesis and GLUT on the circulating AA

To test the possible involvement of *de novo* synthesis of AA in the mechanism for the maintenance of the circulating AA, the effect of the enzyme was also investigated with ODS rats that lack the ability to synthesize AA (Figure 3B). At doses higher than 2 units/kg of body weight, PEG–AOase also decreased plasma AA levels in ODS rats in a similar manner as in normal rats. We also studied the possible involvement of glucose transporters in the regeneration of circulating AA using STZ-induced diabetic rats (Figure 3C). Although steady-state levels of plasma AA in STZ-treated rats (30.74 ± 5.53 μM) were lower than those of control rats (57.41 ± 2.57 μM), the dose-dependency of the PEG–AOase-induced decrease in the circulating AA was similar with the two animal groups.

Effect of a high dose of PEG–AOase on plasma and tissue AA levels

Administration of a high dose of PEG–AOase (50 units/kg of body weight) rapidly diminished circulating AA levels (Figure 4). Although the plasma levels of DAA were elevated by PEG–AOase, the extent of their increase was similar to that of animals that were injected with 1 unit of the enzyme/kg of body weight

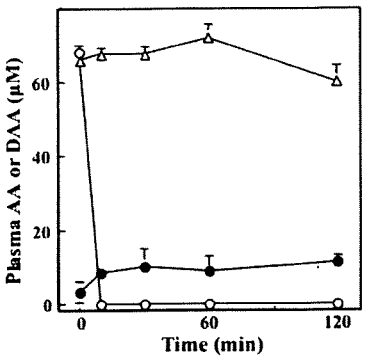

Figure 4 Effect of a high dose of PEG–AOase on the circulating AA and DAA

After intravenous administration of 50 units of PEG–AOase/kg of body weight to normal rats, plasma levels of AA (○, △) and DAA (●) were determined in control (△) and PEG–AOase-treated rats (○, ●). The control animals were treated with the same volume of saline (1 ml/kg of body weight). Values are means ± S.E.M. ($n = 5 \sim 6$).

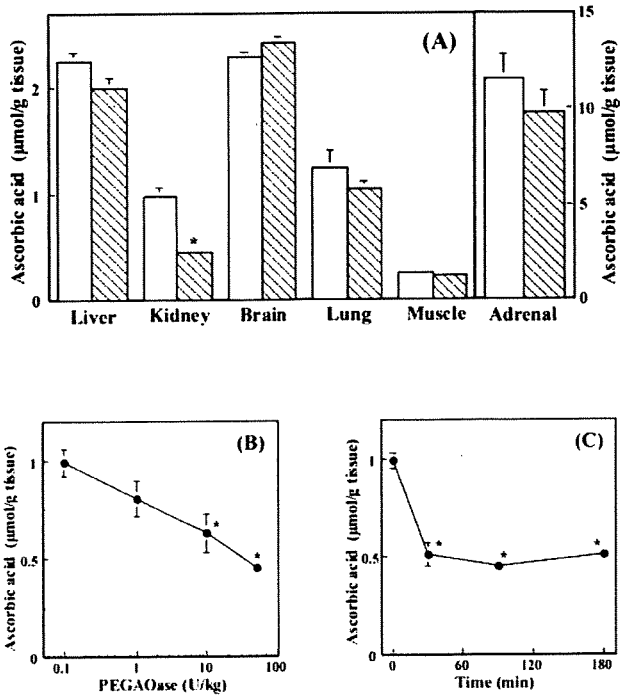

Figure 5 Effect of PEG–AOase on tissue AA levels

PEG–AOase (50 units/kg of body weight) was administered intravenously to normal rats and tissue AA levels were determined after 2 h (**A**) as described in the Materials and methods section. The dose-dependency of the PEG–AOase-induced decrease in renal AA was determined (**B**). Time-dependent changes in renal AA levels were also analysed in animals treated with 50 units of PEG–AOase/kg of body weight (**C**). Values are means ± S.E.M. ($n = 5$). *$P < 0.05$ compared with controls.

(see Figure 2B). Administration of the same doses of the heat-inactivated PEG–AOase had no appreciable effect on the plasma levels of AA and its oxidized metabolites (results not shown). Figure 5 shows the effect of a high dose of PEG–AOase on AA levels in various tissues. Among various tissues examined, AA levels apparently decreased only in the kidney (by approx. 50 %). The decrease in renal AA levels depended on the doses of the enzyme (Figure 5B). A high dose of PEG–AOase (50 units/kg

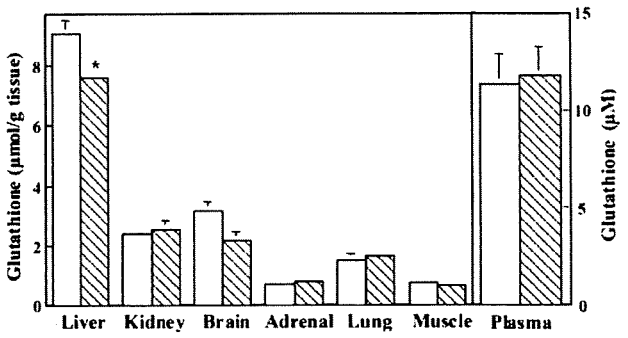

Figure 6 Effect of PEG–AOase on tissue GSH levels

At 2 h after intravenous administration of 50 units of PEG–AOase/kg of body weight to normal rats (hatched columns), total glutathione levels in tissues were determined as described in the Materials and methods section. Control groups (open columns) were administered with 1 ml of saline/kg of body weight. Values are means ± S.E.M. ($n = 5$). *$P < 0.05$ compared with controls.

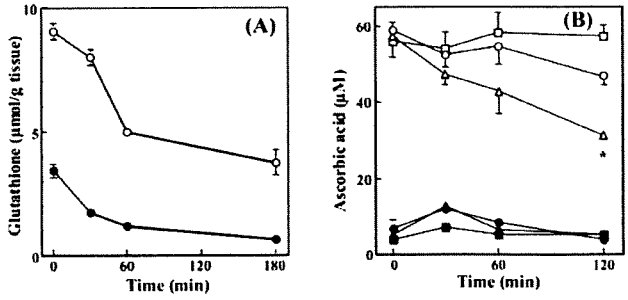

Figure 7 Effect of PEG–AOase on the circulating AA and DAA in BSO-treated animals

After intravenous administration of 1 mmol of BSO/kg of body weight to normal rats, changes in glutathione levels in the liver (○) and kidney (●) were determined (**A**). At 3 h after administration of either saline (○, ●) or BSO (△, ▲), 1 unit of PEG–AOase/kg of body weight was administered to rats. Then, the plasma levels of AA (○, △, □) and DAA (●, ▲, ■) were determined (**B**) as described in the Materials and methods section. Control rats were administered with BSO and saline (□, ■). Most of the glutathione was found to be in the reduced form (GSH). Values are means ± S.E.M. ($n = 5$). *$P < 0.05$ compared with the control.

of body weight) rapidly decreased the renal AA levels by approx. 50 %. The decreased AA levels in the kidney remained unchanged for at least 180 min after the administration of the enzymes (Figure 5C).

Role of GSH in the maintenance of the circulating AA

Since GSH is an important cofactor for the reductive regeneration of AA [24], the effects of PEG–AOase on tissue GSH status were studied (Figure 6). Administration of a high dose of PEG–AOase (50 units/kg of body weight) slightly, but significantly, decreased GSH levels in the liver but not in plasma and other tissues, such as the kidney, brain, adrenal gland, lung and gastrocnemius muscle. To get further insights into the relationship between GSH and AA regeneration, effects of PEG–AOase on plasma AA levels were also observed with BSO-treated rats. Administration of BSO markedly decreased GSH levels in the liver and kidney (Figure 7A). Although administration of 1 unit of PEG–AOase/kg of body weight did not appreciably affect plasma AA levels in control rats, the same dose of the enzyme markedly decreased plasma AA levels in BSO-pretreated rats (Figure 7B). The increased levels of plasma DAA in PEG–AOase-treated animals were similar in the control and BSO-treated groups.

DISCUSSION

The present study demonstrates that AA oxidized in the circulation is reductively regenerated extremely rapidly to maintain its steady-state levels in plasma and that hepatic GSH plays an important role in the regeneration mechanism.

It has been well documented that MDAA rapidly undergoes dismutation to form AA and DAA and the resulting DAA rapidly decomposes to di-keto-L-gulonic acid under physiological conditions [2,4]. Although PEG–AOase rapidly oxidized AA to MDAA both in isolated plasma and blood samples, the amounts of MDAA and DAA formed were fairly small as compared with that of the oxidized AA. Furthermore, both MDAA and DAA disappeared at similar rates (a half-life of 4 min) irrespective of the presence of blood cells. Biochemical analysis revealed that DAA spontaneously decomposed with half-lives of 5 and 4 min in PBS and fresh plasma respectively; most DAA as well as AA oxidized by the enzyme *in vitro* was recovered as oxidative metabolites including di-keto-L-gulonic acid (results not shown). Although di-keto-L-gulonic acid is one of the major oxidation products of AA, MDAA and DAA, it undergoes non-enzymic decomposition to form other metabolites including 3,4-dihydroxy-2-oxobutanal [4]. It should be noted that erythrocytes uptake DAA via GLUT and the transported DAA is subsequently reduced intracellularly to AA [34–36]. Previous studies have also revealed that erythrocytes directly reduce extracellular ascorbate radicals [34,37–39]. Because the transient increase of MDAA in PEG–AOase-treated blood was smaller than that in plasma and the rate of DAA disappearance in plasma and blood were similar (see Figure 1), the two mechanisms for AA regeneration by erythrocytes seem to operate minimally, particularly when plasma AA is oxidized rapidly.

Although a fairly high dose of PEG–AOase (1 unit/kg of body weight) oxidized the circulating AA to form MDAA as effectively as in isolated blood and plasma, it failed to decrease the steady-state levels of plasma AA *in vivo* (compare Figures 1 and 2). Assuming 10 ml for the plasma volume of 200 g rats, the initial concentration of the administered enzyme would be approx. 20 m-units/ml of the circulating plasma; this dose of the enzyme would have been sufficient for rapidly oxidizing the AA in isolated plasma (approx. 60 μM). However, the administration of this dose of the enzyme failed to decrease AA levels in the circulation. Under identical conditions, plasma AA levels decreased rapidly only after isolation of the blood samples from the PEG–AOase-induced animals as observed in *in vitro* experiments with fresh plasma (see Figure 2B), suggesting that the administered enzyme continuously oxidized the circulating AA and the oxidized AA metabolite(s) was reductively regenerated to AA extremely rapidly by some unknown mechanism to maintain its steady-state level in plasma.

To investigate the ability of animals to maintain steady-state levels of the circulating AA, we tested the effect of various doses of a long-acting PEG–AOase. The enzyme started to decrease the circulating AA at doses higher than 2 units/kg of body weight in control, ODS and STZ-treated rats. This observation suggests that the activity of animals to regenerate the circulating AA from its oxidized metabolite(s) for the maintenance of its steady-state levels in plasma is as high as 2 μmol/min per kg of body weight.

Because PEG–AOase dose-dependently decreased the circulating AA in control, ODS and STZ-treated rats in a similar fashion, *de novo* synthesis of AA and uptake of DAA by a GLUT system followed by its intracellular reduction may not account for the rapid regeneration of the circulating AA from its oxidized metabolite(s) (particularly when the rate of AA oxidation is high). It should be noted that, although the dose-dependency of the enzyme to decrease the circulating AA in STZ-treated rats was similar to that of control animals, the steady-state levels of plasma AA in the former (30.7 ± 5.5 μM) were significantly lower than those of the latter (57.4 ± 2.6 μM). This observation is consistent with the findings that plasma AA levels in patients with diabetes mellitus are lower than those of healthy subjects [40]. Thus the activity to scavenge toxic free radicals in and around the circulation would be decreased in diabetic subjects. Alternatively, the generation of reactive oxygen species would be increased in diabetic subjects, thereby resulting in low steady-state levels of the circulating AA.

The steady-state levels of AA in the circulation remained unchanged even in the presence of PEG–AOase (1 unit/kg of body weight) sufficient for decreasing AA levels in fresh plasma. Biochemical analysis revealed that PEG–AOase selectively decreased renal AA levels in a dose-dependent manner with a concomitant decrease of the circulating AA (see Figure 5). When the circulating AA was depleted by a high dose of PEG–AOase (50 units/kg of body weight), renal AA levels rapidly decreased by approx. 50 % and remained at low levels for 180 min. Assuming 1 g for the renal weight of 200 g rats, approx. 17 nmol of renal AA would have been consumed within 1 min in animals administered with 50 units of the enzyme/kg of body weight. This amount of AA is identical with that of plasma AA that could be filtered by the glomerulus [41]. Since bilateral nephrectomy did not affect plasma levels of AA and administration of PEG–AOase dose-dependently decreased plasma AA levels similarly in control and nephrectomized rats (results not shown), the kidney may not play a major role in the reductive regeneration of AA, although the renal AA level depends on its plasma levels. It is not clear at present why renal AA did not decrease to lower levels than 50 % even if extremely high doses of PEG–AOase were administered. It has been well documented that AA and DAA are transferred across plasma membranes of various cells and tissues via active SVCT [42] and bidirectional GLUT systems [43–46] respectively. To our surprise, the levels of AA in liver, brain, lung, muscle and adrenal gland remained unchanged even after depletion of plasma AA (see Figure 5). This observation suggests the presence of a special mechanism that maintains the steady-state levels of cellular AA in these tissues. In contrast, the renal level of AA was affected significantly by PEG–AOase. It should be noted that most low-molecular-mass nutrients filtered by the glomerulus, such as glucose and amino acids, are reabsorbed across renal tubule cells by some transepithelial transport systems in the kidney [41]. Because renal proximal tubules are highly enriched with both SVCT [42] and GLUT [43–46], the filtered AA and DAA would be reabsorbed and transferred to the circulation to maintain their steady-state levels in the kidney and plasma. Thus the renal AA level seems to reflect the balance between the two systems, the one utilized AA within the kidney and the other utilized AA derived from plasma via glomerular filtration (and/or peritubular) mechanism and transepithelial transport to the circulation (salvage system). Depression of plasma AA might decrease not only glomerular filtration of AA (and DAA) but also renal accumulation of the two metabolites. The decreased levels of AA in PEG–AOase-treated animals suggests the importance of the filtered AA and DAA for the maintenance of their steady-state-levels in the kidney. It should be noted that the renal levels of AA remained unchanged after 30 min of PEG–AOase administration. Since most of the nutrients including AA are reabsorbed effectively by renal brush border membranes of proximal tubules, the filtered AA and DAA may not affect their steady-state levels in the lower portions of nephrons than proximal tubules, such as Henle's loop, distal tubules and collecting ducts.

Thus the dynamic aspects of metabolism and transport of AA and DAA at proximal tubules and the lower portion(s) of nephron structures seem to differ; they occur rapidly in the former and slowly in the latter. The possible presence of such zonation of metabolism and transport of AA and DAA within nephron structure should be studied further.

The reductive regeneration of AA from its oxidized forms requires reducing cofactors, such as NAD(P)H and GSH [19,21]. Because both GSH and NAD(P)H are localized ubiquitously with high concentrations, most cells and tissues may have sufficient capacity to catalyse the reductive regeneration of AA. It should be noted, however, that administration of a high dose of PEG–AOase (50 units/kg of body weight) slightly, but significantly, decreased GSH levels in the liver (Figure 6). Under identical conditions, PEG–AOase had no appreciable effect on AA levels in tissues except for the kidney. Thus hepatic GSH might play important roles in the maintenance of the circulating AA. To test this possibility, we investigated the effect of BSO, a specific inhibitor of GSH synthesis, on the steady-state levels of the circulating AA in animals treated with PEG–AOase. When hepatic GSH levels had been decreased by BSO, PEG–AOase (1 unit/kg of body weight) significantly decreased AA levels in the circulation (see Figure 7B). Thus hepatic GSH seems to be responsible, at least in part, for the reductive regeneration of AA from its oxidized metabolite(s) in the circulation. In this context, the presence of a transmembranous enzyme that catalyses the reduction of ascorbate free radicals has been described in hepatocytes, neuronal cells and red blood cells [34,47–49]. It has also been reported that treatment of erythrocytes with *N*-ethylmaleimide at concentrations sufficient for alkylating most intracellular GSH increased the concentration of extracellular ascorbate radicals [38]. Although AA levels in fresh plasma and blood were similarly decreased by a low dose of PEG–AOase, the transient increase of MDAA, but not DAA, was slightly lower in the latter than in the former (see Figure 1). Thus the transmembranous enzyme in the liver and erythrocytes to reduce MDAA to AA may also operate, at least in part, to regenerate the circulating AA. Since the rates of AA decrease by PEG–AOase were similar with isolated blood and plasma samples, hepatic GSH seems to play predominant roles in the regeneration of the circulating AA. A transmembrane mechanism to catalyse the GSH-dependent reduction of MDAA to form AA, similar to that of the NADH-dependent reductase, might operate in the liver. This possibility should be studied further.

Because DAA is unstable and irreversibly decomposed to form di-keto-L-gulonic acid, reductive regeneration of AA from MDAA might be of critical importance for the maintenance of AA levels in the circulation irrespective of the ability of animals to synthesize AA, a potent antioxidant that protects aerobic life from oxidative stress.

AUTHOR CONTRIBUTION

Emiko Kasahara, Misato Kashiba, Mika Jikumaru, Daisuke Kuratsune, Kumi Orita, Yurika Yamate and Kenjiro Hara performed the study. Atsuo Sekiyama and Eisuke Sato contributed to this study with their critical discussion and suggestion. Masayasu Inoue provided most of the ideas of the experiments and his grant supported the study.

FUNDING

This work was supported by the Special Coordination Funds for Promoting Science and Technology from the Ministry of Education, Culture, Sports, Science, and Technology, Japan [project numbers 16590252, 14370062]; and the 21st Century COE Program 'Base to Overcome Fatigue' supported by the Ministry of Education, Culture, Sports, Science, and Technology, Japan.

REFERENCES

1 Niki, E. (1987) Interaction of ascorbate and α-tocopherol. Ann. N Y Acad. Sci. **498**, 186–199
2 Winkler, B. S. (1987) *In vitro* oxidation of ascorbic acid and its prevention by GSH. Biochim. Biophys. Acta **925**, 258–264
3 Frei, B., Stocker, R. and Ames, B. N. (1988) Antioxidant defenses and lipid peroxidation in human blood plasma. Proc. Natl. Acad. Sci. U.S.A. **85**, 9748–9752
4 Nishikawa, Y., Toyoshima, Y. and Kurata, T. (2001) Identification of 3,4-dihydroxy-2-oxo-butanal (L-threosone) as an intermediate compound in oxidative degradation of dehydro-L-ascorbic acid and 2,3-diketo-L-gulonic acid in a deuterium oxide phosphate buffer. Biosci. Biotechnol. Biochem. **65**, 1707–1712
5 Kunitomo, R., Miyauchi, Y. and Inoue, M. (1992) Synthesis of a cytochrome *c* derivative with prolonged *in vivo* half-life and determination of ascorbyl radicals in the circulation of the rat. J. Biol. Chem. **267**, 8732–8738
6 Koyama, K., Takatsuki, K. and Inoue, M. (1994) Determination of superoxide and ascorbyl radicals in the circulation of animals under oxidative stress. Arch. Biochem. Biophys. **309**, 323–328
7 Inoue, M. and Koyama, K. (1994) *In vivo* determination of superoxide and vitamin C radicals using cytochrome *c* and superoxide dismutase derivatives. Methods Enzymol. **234**, 338–343
8 Burns, J. J. (1957) Missing step in man, monkey and guinea pig required for the biosynthesis of L-ascorbic acid. Nature **180**, 553
9 Majumder, P. K., Banerjee, S. K., Roy, R. K. and Chatterjee, G. C. (1973) Effect of insulin on the metabolism of L-ascorbic acid in animals. Biochem. Pharmacol. **22**, 759–761
10 Nishikimi, M. and Yagi, K. (1996) Biochemistry and molecular biology of ascorbic acid biosynthesis. Subcell. Biochem. **25**, 17–39
11 Linster, C. L. and Van Schaftingen, E. (2006) Glucuronate, the precursor of vitamin C, is directly formed from UDP-glucuronate in liver. FEBS J. **273**, 1516–1527
12 Upston, J. M., Karjalainen, A., Bygrave, F. L. and Stocker, R. (1999) Efflux of hepatic ascorbate: a potential contributor to the maintenance of plasma vitamin C. Biochem. J. **342**, 49–56
13 Daruwala, R., Song, J., Koh, W. S., Rumsey, S. C. and Levine, M. (1999) Cloning and functional characterization of the human sodium-dependent vitamin C transporters hSVCT1 and hSVCT2. FEBS Lett. **460**, 480–484
14 Tsukaguchi, H., Tokui, T., Mackenzie, B., Berger, U. V., Chen, X. Z., Wang, Y., Brubaker, R. F. and Hediger, M. A. (1999) A family of mammalian Na^+-dependent L-ascorbic acid transporters. Nature **399**, 70–75
15 Wang, Y., Mackenzie, B., Tsukaguchi, H., Weremowicz, S., Morton, C. C. and Hediger, M. A. (2000) Human vitamin C (L-ascorbic acid) transporter SVCT1. Biochem. Biophys. Res. Commun. **267**, 488–494
16 Liang, W. J., Johnson, D. and Jarvis, S. M. (2001) Vitamin C transport systems of mammalian cells. Mol. Membr. Biol. **18**, 87–95
17 Mackenzie, B., Illing, A. C. and Hediger, M. A. (2008) Transport model of the human Na^+-coupled L-ascorbic acid (vitamin C) transporter SVCT1. Am. J. Physiol. Cell. Physiol. **294**, C451–C459
18 Vera, J. C., Rivas, C. I., Fischbarg, J. and Golde, D. W. (1993) Mammalian facilitative hexose transporters mediate the transport of dehydroascorbic acid. Nature **364**, 79–82
19 Del Bello, B., Maellaro, E., Sugherini, L., Santucci, A., Comporti, M. and Casini, A. F. (1994) Purification of NADPH-dependent dehydroascorbate reductase from rat liver and its identification with 3 α-hydroxysteroid dehydrogenase. Biochem. J. **304**, 385–390
20 May, J. M., Mendiratta, S., Hill, K. E. and Burk, R. F. (1997) Reduction of dehydroascorbate to ascorbate by the selenoenzyme thioredoxin reductase. J. Biol. Chem. **272**, 22607–22610
21 Wells, W. W., Xu, D. P., Yang, Y. F. and Rocque, P. A. (1990) Mammalian thioltransferase (glutaredoxin) and protein disulfide isomerase have dehydroascorbate reductase activity. J. Biol. Chem. **265**, 15361–15364
22 Maellaro, E., Del Bello, B., Sugherini, L., Santucci, A., Comporti, M. and Casini, A. F. (1994) Purification and characterization of glutathione-dependent dehydroascorbate reductase from rat liver. Biochem. J. **301**, 471–476
23 Ishikawa, T., Casini, A. F. and Nishikimi, M. (1998) Molecular cloning and functional expression of rat liver glutathione-dependent dehydroascorbate reductase. J. Biol. Chem. **273**, 28708–28712
24 Inoue, M. (1984) [Inter-organ metabolism and transport of glutathione]. Tanpakushitsu Kakusan Koso **29**, 695–707
25 Tanaka, K., Hashimoto, T., Tokumaru, S., Iguchi, H. and Kojo, S. (1997) Interactions between vitamin C and vitamin E are observed in tissues of inherently scorbutic rats. J. Nutr. **127**, 2060–2064
26 Ogiri, Y., Sun, F., Hayami, S., Fujimura, A., Yamamoto, K., Yaita, M. and Kojo, S. (2002) Very low vitamin C activity of orally administered L-dehydroascorbic acid. J. Agric. Food Chem. **50**, 227–229